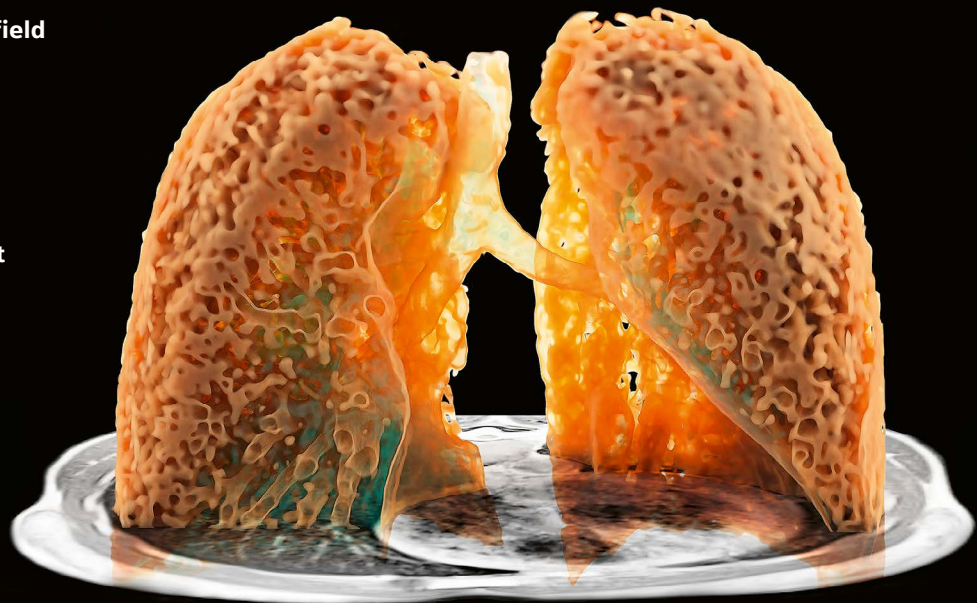


MAGNETOM Flash

MAGNETOM Free.Max special issue USA Edition

siemens-healthineers.us/magnetom-world

- > Page 2
Editorial Comment
Michael Uder, Frederik B. Laun, Armin M. Nagel
- > Page 6
Revisiting the Physics behind MRI and the Opportunities that Lower Field Strengths Offer
André Fischer
- > Page 11
The Next Generation – Advanced Design Low-field MR Systems
Val M. Runge, Johannes T. Heverhagen
- > Page 20
Brain MRI in an Emergency Department
Vincent Dunet, et al.
- > Page 26
Iterative Denoising Applied to 3D SPACE CAIPIRINHA
Alexis Vaussy, Thomas Troalen, et al.
- > Page 35
Autopilot Assistance System for Easy Scanning
Tanja Dütting, Stephan Clasen
- > Page 39
A Brief History of the DryCool Magnet Development
Simon Calvert





Professor Dr. med. Michael Uder graduated from Saarland University in 1992. He trained in radiology and subsequently became Professor of Radiology at Friedrich-Alexander-University Erlangen-Nürnberg, Germany. Since 2009, Professor Uder has led the Institute of Radiology.

Professor Dr. Frederik Laun and **Professor Dr. Armin Nagel** both head MRI physics research groups at the Institute of Radiology. Professor Laun has a strong research focus on diffusion-weighted imaging and quantitative susceptibility-weighted imaging. The research interests of Professor Nagel are predominantly in ultra-high field and non-proton MRI.

Dear readers and colleagues,

We have been asked to introduce this RSNA edition of MAGNETOM Flash by talking about the possibilities of high-performance, 0.55 Tesla magnetic resonance imaging (MRI). At first glance, a move to lower field strengths seems to be counterintuitive, given the fact that there have been tremendous efforts during the past decades to design MRI systems with higher magnetic field strengths. Undoubtedly, many diagnostic imaging applications clearly benefit from high magnetic field strengths such as 3T or even 7T. The latter has become a clinical field strength with the clinical approval of the MAGNETOM Terra system in 2017. MRI at 7T enables unprecedented spatial resolution, improved spectral resolution, and efficient detection of non-proton nuclei such as sodium and phosphorous. Therefore, a number of diagnostic applications – particularly neurological and musculoskeletal imaging – clearly benefit from ultra-high-field MRI [1]. In addition, most methodology-oriented MRI research is currently being performed at field strengths $\geq 3T$ [2].

However, lower field strength MRI ($< 1T$) could potentially benefit from many of the technical developments that have been achieved at higher field strengths [3]. Several articles in this edition cover a broad range of new technical innovations that also enable high-performance MRI at low field strengths. Here, advanced-design, low-field systems and innovative magnet designs, as presented by Val Runge and colleagues (page 11) and Simon Calvert (page 44), will not only contribute to improved image

quality, but will also facilitate installation and improve accessibility and reach of MRI.

Sophisticated algorithms and artificial intelligence (AI) are now aiding slice positioning, and as image reconstruction increasingly involves AI and deep learning, we can expect to see more developments in the future that will further mitigate concerns about reduced image quality at lower field strengths. Alexis Vaussy et al. combined parallel imaging acceleration with a modern iterative denoising reconstruction algorithm (page 26). For 3D neuroimaging, they achieved submillimeter spatial resolution at 3T in clinically acceptable acquisition times, this is usually only feasible at ultra-high magnetic field strengths. In addition, some MRI-guided interventions might become possible at low field strength, largely due to reduced device heating as compared to field strengths $\geq 1.5T$ [4].

Thus, imaging at higher field strengths is not always advantageous (see also André Fischer on page 6). Although 1.5T and 3T MRI systems have replaced older low-field systems ($< 1T$) in most hospitals, low-field MRI has regained popularity over the past few years [5]. At higher field strengths, susceptibility artifacts increase, imaging near implants is challenging or in some cases even impossible, and last but not least, installation costs increase with magnetic field strength. One benefit of low-field systems is their cost-effectiveness: Compared with conventional 1.5T, 3T, or 7T systems, the costs of manufacturing, transporting, and operating the scanner



In the future, 0.55T MRI will hopefully help to increase accessibility to MRI examinations for many patients and could potentially be used for identifying patients that require dedicated examinations in high- or ultra-high-field systems. Therefore, MRI systems at all field strengths will contribute to high-end imaging and optimal patient care.

and its magnet are much lower. MRI is one of the most advanced and versatile diagnostic imaging modalities available today, yet this also renders it one of the most expensive – both in terms of initial investment and the lifetime running costs. This is partly due to the high structural demands that accompany the installation of an MRI system. In addition to needing a large amount of space and very strong floors, hospitals also have to arrange for the installation of major components such as quench pipes. This limits access to MRI examinations not only in developing countries, but also in smaller, poorly funded hospitals.

Costs can be reduced by reducing hardware costs and by simplifying infrastructure requirements. MAGNETOM Free.Max benefits from the new DryCool magnet technology, where the magnet is fully sealed and only requires 0.7 liters of helium. This means, there is no need for helium refills, and no quench pipe is required.

In addition to the accessibility issues mentioned, access to MRI is also often limited by the availability of qualified staff. This is true everywhere, including in industrialized nations, where shortages of MRI technologists are a frequent problem. Thus, there is a need for true push-button workflows based on sophisticated, intelligent automation. As presented by Tanja Dütting et al. (page 40), autopilot systems will allow users to perform what were previously complex and error-prone MRI examinations at the touch of a single button. At the same time, it is important that there remains access to a state-of-the-art

user interface that enables advanced settings and a high degree of flexibility for more experienced technologists.

Choosing the counterintuitive route and going lower instead of higher will offer clinical benefits for many applications: Longer T2* relaxation times will reduce blurring artifacts for echo-planar imaging (EPI) readouts (e.g., in diffusion scans), and will also enable improved MRI of tissues and organs with short relaxation times, such as tendons and the lung. The specific absorption rate (SAR) can be much lower, which will also enable safer imaging of implants. In addition, the reduction in susceptibility artifacts will enable improved passive metal implant imaging.

At University Hospital Erlangen, we operate MRI systems with field strengths of 0.55T, 1.5T, 3T, and 7T. We are convinced that – at least for large centers such as university hospitals that have to cover the whole range of diagnostic applications – there is not merely one “optimal” magnetic field strength that fits best for all scenarios. Some patients will benefit from imaging at 3T or even 7T. However, for most patients, diagnostic quality at 1.5T or 0.55T will most likely be sufficient. For some applications (e.g., lung imaging, imaging near implants, and interventions), low-field MRI might even enable improved image quality. In the future, low-field MRI will hopefully help to increase accessibility to MRI examinations for many patients and could potentially be used for identifying patients that require dedicated examinations in high- or ultra-high-field systems. Therefore, MRI systems at all field strengths will contribute to high-end imaging and optimal

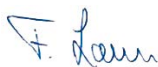
patient care. Furthermore, close collaboration between radiologists, manufacturers, and basic scientists such as MRI physicists and data scientists is crucial for further expanding the diagnostic possibilities of MRI at all field strengths.

We hope that the new 0.55T MAGNETOM Free.Max platform will provide more people with access to MRI examinations (e.g., in developing countries and emerging markets). Even for industrialized countries, the factors mentioned above can restrict the flexibility necessary to provide MRI where it is needed – at the point of care in emergency departments (see also, e.g., the work of Vincent Dunet and associates (page 20), in rural community hospitals, and in orthopedic practices and the like.

We hope you enjoy reading this issue!



Michael Uder



Frederik B. Laun



Armin M. Nagel

References

- 1 Ladd ME, Bachert P, Meyerspeer M, Moser E, Nagel AM, Norris DG, Schmitter S, Speck O, Straub S, Zaiss M. Pros and cons of ultra-high-field MRI/MRS for human application. *Prog Nucl Mag Res Sp* 2018; 109: 1-50.
- 2 Hanspach J, Nagel AM, Hensel B, Uder M, Koros L, Laun FB. Sample size estimation: Established practice and considerations for original investigations in MRI technical development studies. *Magn Reson Med* 2020; (online ahead of print) doi: 10.1002/mrm.28550
- 3 Marques JP, Simonis FFJ, Webb AG. Low-field MRI: An MR physics perspective. *J Magn Reson Imaging* 2019; 49(6): 1528-1542.
- 4 Campbell-Washburn AE, Ramasawmy R, Restivo MC, Bhattacharya I, Basar B, Herzka DA, Hansen MS, Rogers T, Bandettini WP, McGuirt DR, Mancini C, Grodzki D, Schneider R, Majeed W, Bhat H, Xue H, Moss J, Malayeri AA, Jones EC, Koretsky AP, Kellman P, Chen MY, Lederman RJ, Balaban RS. Opportunities in Interventional and Diagnostic Imaging by Using High-Performance Low-Field-Strength MRI. *Radiology* 2019; 293(2): 384-393.
- 5 Sarraçanie M, LaPierre CD, Salameh N, Waddington DEJ, Witzel T, Rosen MS. Low-Cost High-Performance MRI. *Sci Rep* 2015; 5: 15177.

We appreciate your comments.

Please contact us at magnetomworld.team@siemens-healthineers.com

Editorial Board



Antje Hellwich
Editor-in-chief



Rebecca Ramb, Ph.D.
Vice President of MR
Research & Clinical Translation



Nadine Leclair, M.D.
MR Medical Officer



Wellesley Were
MR Business Development
Manager Australia and
New Zealand



Jane Kilkeny
Vice President of MR
Malvern, PA, USA



Dr. Sunil Kumar Suguru Laxman
Clinical & Product Specialist MRI
Dubai, United Arab Emirates

Review Board

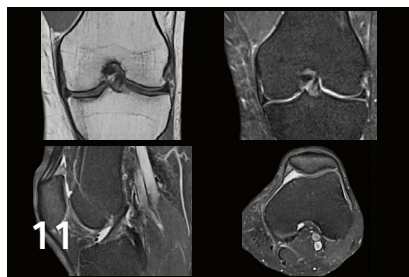
André Fischer, Ph.D.
Global Segment Manager Neurology

Daniel Fischer
Head of Clinical and Scientific
Marketing

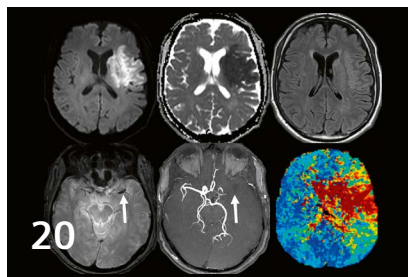
Giulia Ginami, Ph.D.
Global Product Manager PET-MRI

Heiko Meyer, Ph.D.
Head of Neurology Predevelopment

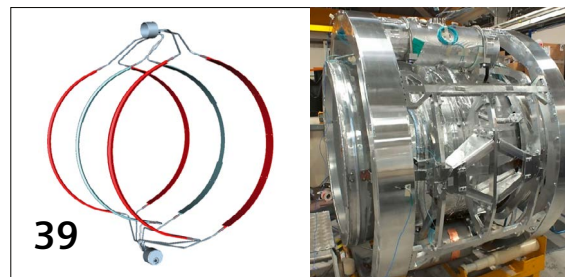
Gregor Thörmer, Ph.D.
Head of Oncology Predevelopment



The next generation –
advanced design low-field MRI



Brain MRI in an emergency department



DryCool magnet development

Editorial Comment

- > 2 **Editorial Comment**
Michael Uder, Frederik B. Laun, Armin M. Nagel
University Hospital Erlangen, Germany

- > 26 **Iterative Denoising Applied to 3D SPACE CAIPIRINHA: A New Approach to Accelerate 3D Brain Examination in Clinical Routine**
Alexis Vaussy, Thomas Troalen, et al.
Siemens Healthineers, Saint-Denis, France

Physics

- > 6 **Revisiting the Physics behind MRI and the Opportunities that Lower Field Strengths Offer**
André Fischer
Siemens Healthineers, Erlangen, Germany

Technology

- > 35 **Experience of Using a New Autopilot Assistance System for Easy Scanning in Brain and Knee MRI Examinations**
Tanja Dütting, Stephan Clasen
Institute for Diagnostic and Interventional Radiology, Kreiskliniken Reutlingen, Germany
- > 39 **MAGNETOM Free.Max: from Concept to Product, a Brief History of the DryCool Magnet Development**
Simon Calvert
Siemens Healthineers, Oxford, UK

Head-to-Toe Imaging

- > 11 **The Next Generation – Advanced Design Low-field MR Systems**
Val M. Runge, Johannes T. Heverhagen
University Hospital of Bern, Inselspital, University of Bern, Switzerland

About Siemens Healthineers

- > 44 **Our purpose**

Neurological Imaging

- > 20 **Brain MRI in an Emergency Department: Clinical Implementation and Experience in the First Year**
Vincent Dunet, et al.
Lausanne University Hospital and University of Lausanne, Switzerland

MAGNETOM Free.Max is currently under development and is not for sale in the U.S. and in other countries. Its future availability cannot be ensured.

Revisiting the Physics behind MRI and the Opportunities that Lower Field Strengths Offer

André Fischer, Ph.D.

Global Segment Manager Neurology, Siemens Healthineers, Erlangen, Germany

This article outlines why moving to higher magnetic fields may not always be advantageous in MRI. We focus on phenomena that have a substantial impact on daily routine, and aim to provide a solid insight into underlying physical mechanisms. Some discussions have been simplified in the interest of addressing a broad range of readers.

Introduction

When MRI first transitioned from research into clinical practice in the early 1980s, typical magnetic fields were between 0.2 and 0.5T, mainly due to technical limitations. The clinical MRI community quickly moved towards higher fields, converging on 1.5T, which became the new standard. Later, around the turn of the millennium, 3T magnets started to penetrate the market, fueled by the quest for higher signal to noise ratio (SNR) with higher field strength. Today, 1.5T and 3T are the clinical workhorses, present in almost every large hospital radiology department. Lately, Siemens Healthineers have pushed for even higher field, introducing the MAGNETOM Terra – the first clinical 7T scanner with FDA clearance.

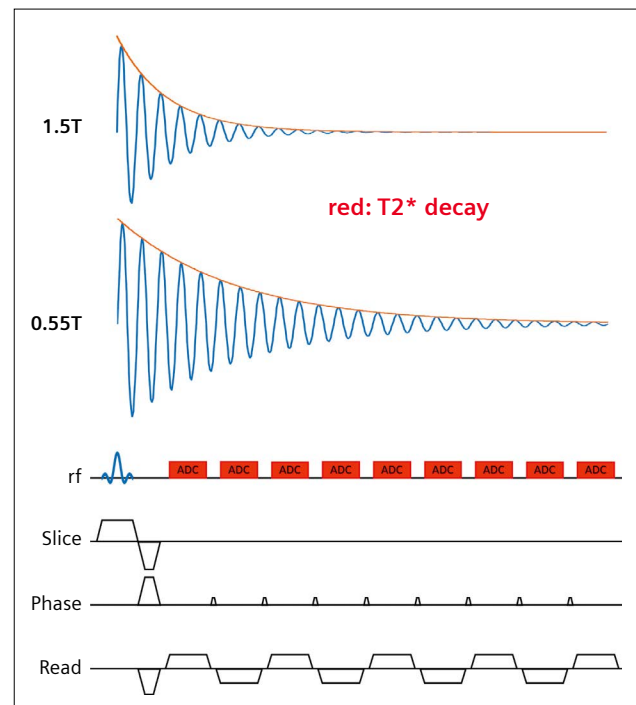
There was an immediate clinical advantage in moving to higher field. It increases the magnetization available for imaging, which improves SNR. The increased signal can be invested into either higher spatial resolution or reduced imaging time. For human MR imaging in general, SNR increases linearly with the field [1]. However, in order to maintain image quality, the chemical shift between different nuclei can be kept constant by adjusting the receiver bandwidth, in which case SNR is proportional to the square root of the field [1, 2]. Recent research in ultra-high-field human brain MRI suggests faster than linear increase of SNR with field [3].

Then again, there is no such thing as a free lunch. Increasing the field increases radiofrequency absorption in tissue, increases artifacts, and degrades imaging in various other ways, through the physical phenomena described below.

Radiofrequency absorption

MRI scanners use high-power radiofrequency pulses to manipulate nuclear spins. This RF energy would become a health hazard if it were intense enough to overheat tissue, so scans have to stick to safety limits.

Specific absorption rate (SAR) is the relevant measure of RF absorption, in watts per kilogram of body tissue. The International Electrotechnical Commission [4] sets maximum SAR of 2 W/kg in normal mode, and of 4 W/kg in first-level mode (both for whole-body SAR averaged over 6 minutes).



1 During a typical EPI gradient echo readout, the later echoes suffer from low signal intensity at 1.5T compared with 0.55T, and the resulting images are blurred (see Figure 2). The red envelope in the upper two sinusoids corresponds to the observed T2* decay (neglecting gradient-induced dephasing).

The absorbed energy depends on the square of the field, so it increases by a factor of 4 when doubling the field. Most clinicians and researchers have faced SAR limitations, e.g., in SAR “heavy” examinations such as Cardio or MSK, especially with the advent of 3T scanners in clinical routine. Operating in first-level mode is often mandatory at 3T, but even then the SAR threshold limits the use of clinically relevant sequences.

Using 0.55T instead of 1.5T or 3T reduces SAR by a factor of 7.5 or 30, respectively. Consequently, many SAR-intense sequences, e.g., TrueFISP or TSE, do not hit the SAR limit at 0.55T. This can help increase SNR by applying higher flip angles (e.g., 180° instead of lower flip angles such as 150° at 3T for TSE imaging; 90° flip angle for TrueFISP possible), or shortening radiofrequency (RF) pulses to minimize echo time (TE) and TR.

Relaxation times

The relaxation of spins is the main mechanism for the observed image contrast in MRI. In this section, we will review the types of relaxation and their impact on clinical routine.

T1 relaxation

The spin of a proton gives it a magnetic moment. Just as a compass needle aligns with the magnetic field of the Earth, the proton spin tends to align parallel to an external magnetic field B_0 ; this is the lower energy state of the proton spin, while the anti-parallel state is higher energy. In an MRI, a radiofrequency pulse can be used to convert parallel proton spins to their anti-parallel state; then spin-lattice relaxation (also known as T1 relaxation) gradually brings them back to their energetically preferred parallel state.

This is triggered by the random magnetic field fluctuations – sometimes referred to as “magnetic noise” – of the surrounding magnetic moments caused by, e.g., protons, electrons, and various molecules. The energy difference between the parallel and anti-parallel state corresponds to a resonance frequency, proportional to the field, and relaxation is triggered by “magnetic noise” close to that frequency. Generally speaking, this “noise” at lower frequencies is stronger than at higher frequencies – so at lower field, relaxation is more efficient.

The time constant of this relaxation, T1, is defined by [5]

Equation 1

$$T1 \propto \frac{B_0^b}{a}$$

with constants a and b that must be determined by experiment. Recent investigations [6] across a range of clinical fields (0.55T, 1.5T, 3T, 7T) revealed the following linear dependency between T1 and B_0 :

Equation 2

$$T1 \propto \frac{B_0}{12.2}$$

with a = 12.2 and b = 1. This means that T1 gets shorter if the field decreases.

How does this help us from a clinical point of view? If T1 is shorter, the repetition time (TR) can be reduced, resulting in decreased scan time. For example, T1 for gray matter decreases from 1000–1300 ms at 1.5T down to 700–800 ms at 0.55T [7]. Due to this, TR can be reduced by the same proportion, at least 25%.

We can address the loss of SNR by averaging. SNR scales with the square root of the field [1, 2], so to have SNR at 0.55T comparable to that at 1.5T, three averages are necessary. Instead of tripling your imaging time, it will only increase your scan time by a factor of 2.25 because TR could be selected 25% shorter than at 1.5T. Physics comes in favorably from the T1 perspective at lower field strength.

T2 relaxation

Spin-spin relaxation, commonly referred to as transverse or T2 relaxation, does not show high dependency on field.

To observe T2 relaxation, a radiofrequency pulse first flips proton spins so that their net magnetization is perpendicular to the external field. Magnetization then precesses around the B_0 direction at the Larmor frequency

Equation 3

$$\omega = \gamma \cdot B_0$$

where γ is the gyromagnetic ratio of the proton.

The RF pulse also puts proton spins in phase. Gradually, magnetic noise knocks some spins out of phase, which decreases the net magnetization (the vector sum of all spins). After time T2 magnetization decreases by a factor of e, so after approximately 5T2 it has effectively vanished. By this argument the strength of the field does not affect T2 relaxation.

Nonetheless, empirical research shows that T2 increases slightly as the field falls. For gray matter, T2 values at 1.5T are 90–110 ms, while at 0.55T they are 110–120 ms

[5]. This would allow turbo spin echo (TSE) imaging to employ longer echo trains at 0.55T, reducing the number of required readouts, potentially reducing the required scan time compared with 1.5T – if the SNR penalty is neglected.

T2* relaxation

Imaging the diffusion of water molecules is one phenomenon that often relies on T2* contrast, and other applications such as BOLD imaging and DSC neuro perfusion suffer from T2* loss or blurring as well. All gradient-echo readouts, such as echo planar imaging (EPI), are modulated by T2* decay.

Several phenomena are affected by both regular T2 decay and another decay process known as T2'. T2' is caused by static inhomogeneities in the magnetic field, such as susceptibility-induced magnetic field gradients, which combine to form T2* relaxation.

The overall timescale is

Equation 4

$$T2^* = \left(\frac{1}{T2} + \frac{1}{T2'} \right)^{-1}$$

By employing TSE sequences, T2' can be recovered and true T2 decay can be observed.

Susceptibility-induced magnetic field gradients scale with B₀, so at high field T2* is shorter than at low field. In gray matter, T2* at 1.5T is typically 70–80 ms, while at 0.55T it is 80–90 ms [5]. This allows more SNR-efficient

EPI sampling at 0.55T, since the available echo signal amplitude is relatively large for later echoes in the EPI train (see Figure 1). A side effect is reduced blurring (see Figure 2).

Susceptibility

Magnetic susceptibility measures how a material responds to an external magnetic field. The induced magnetization inside a material under external magnetic field strength *H* is:

Equation 5

$$\vec{M} = \chi \vec{H}$$

where χ is magnetic susceptibility¹.

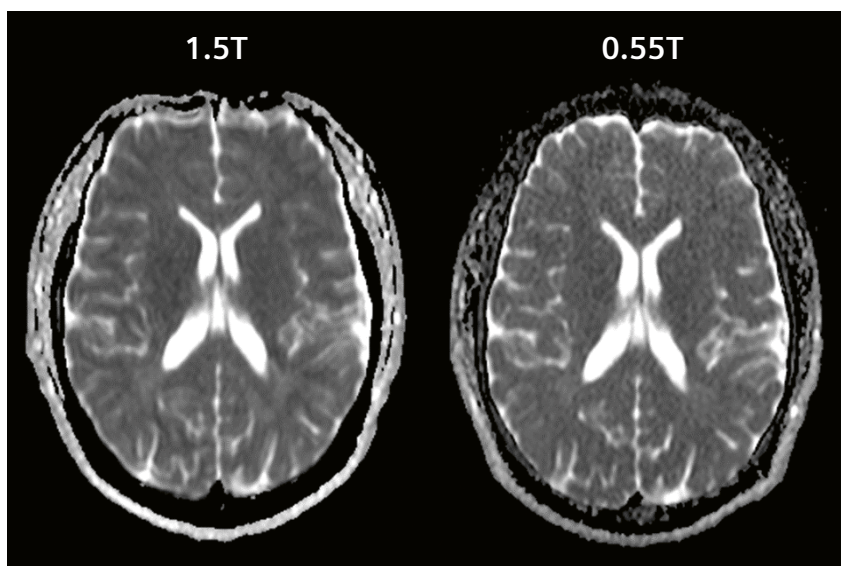
The induced magnetization *M* and the external magnetic field *H* result in the magnetic flux density *B*:

Equation 6

$$\vec{B} = \mu_0 \vec{H} + \vec{M} = (\mu_0 + \chi) \vec{H}$$

where $\mu_0 = 4\pi \cdot 10^{-7}$ is the magnetic permeability of vacuum.

Eq. 6 tells us that as *H* increases, the change in *B* depends on the value of χ . If $\chi > 0$, *B* increases; if $\chi < 0$, *B* decreases; and if $\chi = 0$, *B* doesn't change.



2 Due to faster T2* decay at higher field (see Figure 1), the apparent diffusion coefficient map at 1.5T is slightly blurred along the anterior-posterior direction. This is particularly apparent in the hyperintense gyri. Both images were acquired on the same volunteer. Also, a slight geometric distortion in the anterior brain region is visible at 1.5T (see Susceptibility).

¹There are different physical phenomena behind susceptibility. Diamagnetism is a universal property of any material which decreases the magnetic field inside it. It is often "hidden" underneath the stronger phenomenon of paramagnetism, which increases the magnetic field. Both dia- and paramagnetism can only be observed when an external magnetic field is present. As a side note, ferromagnetism is a property that is maintained even when the external magnetic field has been turned off.

Susceptibility changes can be a valuable contrast source. Susceptibility-weighted imaging (SWI) exploits slight differences in χ to visualize veins in the brain, enabling the diagnosis of cerebral hemorrhage, for example. Quantitative susceptibility mapping (QSM) produces a map of susceptibility that might constitute a new biomarker [8–10].

At the same time, susceptibility is a source of artifacts. Near the sinuses and auditory canal, for example, the changes in susceptibility moving from air to tissue cause geometric distortions in conventional EPI-based imaging, including diffusion-weighted imaging (DWI) and functional MRI (fMRI). Eq. 6 shows that reducing the external field also reduces the absolute differences in local magnetic fields, which makes susceptibility-induced artifacts much less prominent. This can be seen in Figure 3, showing the results of DWI scans on the same volunteer performed on a 3T, a 1.5T, and a 0.55T system. While SNR clearly decreases as field decreases, the geometric distortions are significantly reduced as well.

Diffusion imaging of the optic nerves is also substantially improved at lower field (see Figure 4). A similar behavior is to be expected for imaging of metallic implants such as hip implants. This has been shown in the literature [11–13] and might have a significant impact on clinical practice in the aging societies of industrialized nations.

B_0 and B_1 Homogeneity

B_0 homogeneity is of utmost importance for image quality, and less effort is required to guarantee this homogeneity at lower B_0 values.

B_1 homogeneity is also crucial, to ensure homogenous excitation of the desired slice or volume. B_1 – or more precisely B_1^+ – is the transmitted radiofrequency field that excites the protons at their Larmor frequency. The flip angle is directly related to B_1 through:

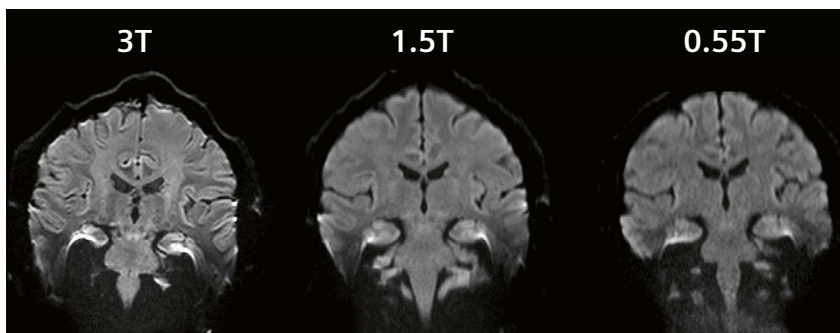
Equation 7

$$\alpha = \gamma \cdot B_1 \cdot t_p$$

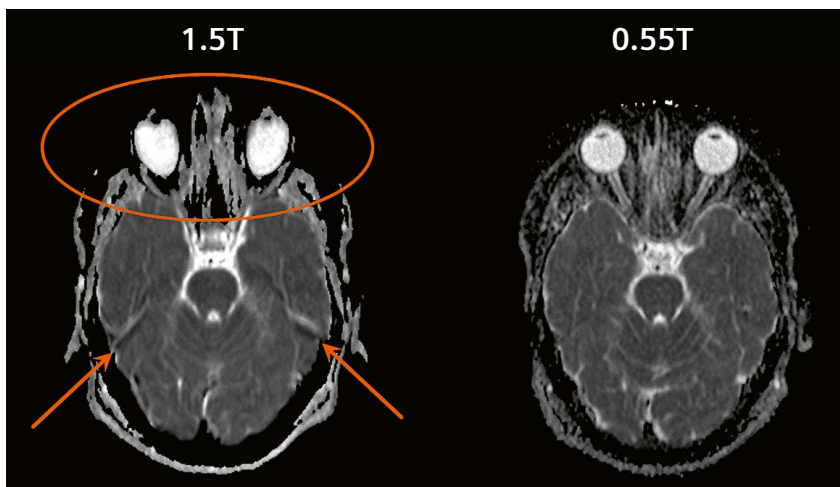
where α is the targeted flip angle of the applied RF pulse, γ is the gyromagnetic ratio of the proton, B_1 is the magnetic field of the applied RF pulse, and t_p is the pulse duration.

From this equation, it is clear that if B_1 is not homogeneous, the excited slice or volume will show varying flip angle, leading to variations in contrast and SNR.

When the Larmor frequency ω increases, the associated wavelength λ decreases. At 3T, the wavelength within the human body is approximately 25–30 cm [14], close to the dimensions of a human torso. This results in construc-



3 Coronal EPI diffusion scans ($b = 1000 \text{ s/mm}^2$) acquired on the same volunteer with three different fields. Moving to lower field typically comes with a reduction in SNR; but at the same time susceptibility artifacts near the temporal lobe due to vicinity of the air-filled internal auditory canal are substantially reduced.



4 Geometric distortions caused by the air-filled sinuses and internal auditory canal are substantially reduced at lower field. In this example on the same volunteer at 1.5 and 0.55T, the eyeballs maintain their almost spherical shape, and the optic nerves are clearly visible (ellipse); the susceptibility artifacts near the temporal lobes (arrows) are almost invisible at 0.55T.



tive and destructive interference within the body, leading to inhomogeneous B_1 excitation. This phenomenon has triggered lots of research efforts to mitigate this problem and can now be considered understood; countermeasures such as B_1 shimming are available, but come with increased costs and hardware requirements.

Conversely, at lower field, the Larmor frequency is lower, so the associated RF wavelength is longer. This reduces or even eliminates the effect of interference. For example, at 0.55T, the wavelength is approximately 130–140cm, much larger than typical body diameter. So B_1 will be more homogeneous at lower field, giving more homogeneous contrast and SNR behavior.

Summary

For more than 20 years, the clinical standard for MR imaging has been either 1.5T or 3T. While many of the physical advantages of low field have been well known in the scientific community, the push for higher SNR favored higher fields. However, in the light of technical improvements made over the last 20 years, other metrics may be favored. Improvements in image reconstruction – from parallel imaging [16,17] and compressed sensing [18] to deep learning [19] – mean that clinicians can make optimal use of the available signal while exploiting the physical advantages of low-field MRI, such as reduced artifacts.

If SNR is sufficient at two different fields, then the focus may fall instead on diagnostic or financial value. Scientific literature even back in the mid 1990s showed no significant difference in diagnostic sensitivity or specificity between 1.5T and lower-field systems [20, 21]. Low-field machines are also less expensive, which is particularly relevant given the cost pressure in many healthcare systems.

All these factors could help bring MRI to places it has not been before – spreading into new geographical and clinical areas. The future of low-field MRI looks bright.

References

- Hoult DI et al. The field dependence of NMR imaging. *Magn Reson Med*. 1986;3:722-746.
- Boska MD et al. Comparison of P-31 MRS and H-1 MRI at 1.5 and 2.0 T. *Magn Reson Med*. 1990;13:228-238.
- Pohmann R et al. Signal-to-noise ratio and MR tissue parameters in human brain imaging at 3, 7, and 9.4 tesla using current receive coil arrays. *Magn Reson Med*. 2016;75:801-809.
- IEC 60601-2-33
- Korb JP, Bryant RG. The physical basis for the magnetic field dependence of proton spin-lattice relaxation rates in proteins. *J Chem Phys*. 2001;115:10964–10974.
- Wang Y et al. B0-field dependence of MRI T1 relaxation in human brain. *Neuroimage*. 2020;213:116700.
- Campbell-Washburn A et al. Opportunities in Interventional and Diagnostic Imaging by Using High-performance Low-Field-Strength MRI. *Radiology* 2010;293:384-393.
- Wang Y, Liu T. Quantitative Susceptibility Mapping (QSM): Decoding MRI Data for a Tissue Magnetic Biomarker. *Magn Reson Med*. 2015;73:82-101.
- Tan H et al. Quantitative Susceptibility Mapping in Cerebral Cavernous Malformations: Clinical Correlations. *Am J Neuroradiol*. 2016;37:1209-1215.
- Zeineddine HA et al. Quantitative susceptibility mapping as a monitoring biomarker in cerebral cavernous malformations with recent hemorrhage. *J Magn Reson Imaging*. 2018;47:1133-1138.
- Gray CF et al. Low-field magnetic resonance imaging for implant dentistry. *Dentomaxillofacial Radiology*. 1998;27:225-229.
- Klein H-M. Clinical Low Field Strength Magnetic Resonance Imaging - A Practical Guide to Accessible MRI. New York: Springer; 2016.
- Klein H-M. Low-Field Magnetic Resonance Imaging; *Fortschr Röntgenstr*. 2020;192:537-548.
- Choi J-Y et al. Abdominal Applications of 3.0-T MR Imaging: Comparative Review versus a 1.5T system. *Radiographics*. 2008;28:e30.
- Moelker A et al. Relationship between magnetic field strength and magnetic-resonance-related acoustic noise levels. *MAGMA*. 2003;16:52-55.
- Pruessmann KP et al. SENSE: sensitivity encoding for fast MRI; *Magn Reson Med*. 1999;42:952-962.
- Griswold MA et al. Generalized autocalibrating partially parallel acquisitions (GRAPPA). *Magn Reson Med*. 2002;47:1202-1210.
- Lustig M et al. Sparse MRI: The application of compressed sensing for rapid MR imaging. *Magn Reson Med*. 2007;58:1182-1195.
- Hammernik K et al. Learning a variational network for reconstruction of accelerated MRI data. *Magn Reson Med*. 2018;79:3055-3071.
- Lee DH et al. MR Imaging Field Strength: Prospective Evaluation of the Diagnostic Accuracy of MR for Diagnosis of Multiple Sclerosis at 0.5 and 1.5T. *Radiology*. 1995;194:257-262.
- Vellet AH et al. Anterior cruciate ligament tear: prospective evaluation of diagnostic accuracy of middle- and high-field-strength MR imaging at 1.5 and 0.5 T. *Radiology*. 1995;197:826-830.

Contact

André Fischer, Ph.D.
Global Segment Manager Neurology
Siemens Healthineers
SHS DI MR M&S CSM
Allee am Roethelheimpark 2
91052 Erlangen, Germany
andre.fischer@siemens-healthineers.com



The Next Generation – Advanced Design Low-field MR Systems

Val M. Runge, M.D.; Johannes T. Heverhagen, M.D., Ph.D.

Department of Diagnostic, Interventional and Pediatric Radiology,
University Hospital of Bern, Inselspital, University of Bern, Switzerland

Low-field superconducting MR systems, operating between 0.35 and 0.6T, were only briefly evaluated for clinical use in the 1980s before they were superseded by higher field systems. An important question today is the potential of such units, operating at a known sweet spot – 0.55T, employing in design all the knowledge gained during the interval decades. Looking at cost, flexibility, image quality, and accessibility, there is a very bright future for advanced design low-field MR units, which should expand markedly, worldwide, the use and clinical value of MR.

A brief history of the evolution of MR field strength for clinical systems

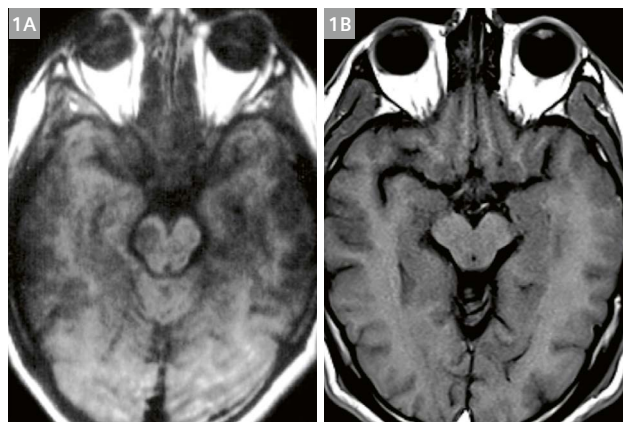
Paul Lauterbur and Peter Mansfield jointly shared the 2003 Nobel Prize in Physiology/Medicine for their fundamental work in the 1970s in the field now known as MRI. Soon thereafter, John Mallard introduced the first whole body MRI system, which operated at a field strength of 0.014T. The potential for improved SNR with higher field strength was quickly recognized, resulting in a second prototype operating at 0.028T, but still utilizing a resistive magnet.

The initial commercial development of clinical MR – in the early 1980s – was led by two companies no longer in existence, Diasonics and Technicare. Both used superconducting magnets, with the first company delivering 0.35T units, and the second company initially 0.5T units (Fig. 1) and subsequently 0.6T units. In the mid 1980s Siemens' first commercial units were delivered. These operated at a field strength of 1.0T, a theoretical optimum defended by many prominent scientists of the day.

In the late 1980s, a marketing blitz by one major manufacturer, who was yet to enter the field, led to all of the major X-ray manufacturers developing 1.5T systems. Standardizing on a field strength of 1.5T was a radical idea, with no clinical systems having been delivered at that time with such a high field strength. Much of the premise for development of this field strength was based on the possible clinical development and utility of techniques

that would be thus enabled, such as phosphorus spectroscopy. This premise later proved largely false. Nevertheless, all the major vendors were forced to invest, largely due to marketing pressure, in the development of clinical 1.5T units. By the 1990s, delivery of 1.5T units dominated the industry.

Then in the 2000s, the debate began concerning 3T, primarily on the basis of brain imaging, which was indeed the only exam of sufficient quality for clinical diagnosis that these early 3T whole body systems could acquire. There were major challenges to make 3T an acceptable scanner, not only for the brain but also for the spine, musculoskeletal system, and body. The prolongation of T1, in plane and through plane chemical shift, and perhaps most prominently patient heating (SAR) all presented major challenges to overcome in making 3T clinically viable. Indeed, despite the very high quality of scans at 3T in many anatomic areas today, the debate continues regarding 1.5T versus 3T. Cost is a major impediment, being substantially greater for 3T in terms of the system itself as well as installation. Reflecting this debate and heavily these costs, today for new MRI units two 1.5T systems are still sold for every 3T.



1 A historical comparison of low field brain imaging in (1A) 1984 (on a Technicare 0.5T scanner) versus (1B) the current 2020 standard. The scan time was reduced from 10 to 4 minutes, accompanied by a marked improvement in SNR and spatial resolution due to interval technologic advances using the MAGNETOM Free.Max system.

MAGNETOM Free.Max is currently under development and is not for sale in the U.S. and in other countries. Its future availability cannot be ensured.

What data exists regarding low-field imaging from the 1980s and 1990s?

The development of 1.5T imaging in the late 1980s occurred despite the lack of substantial evidence at that time, supporting that field strength, for medical diagnosis and sensitivity to disease. More specifically, few large-scale clinical trials exist from that era comparing efficacy at low-field to that at 1.5T. It is to be granted that results today at 1.5T are indeed excellent, but let us turn to the little data that was available comparing field strengths during that era of rapid development.

From the scant scientific literature, two major publications/clinical trials stand out for their comparison of low and high field. These trials cover two important anatomic areas of clinical utility for MR, the brain and the musculoskeletal system. Both provide little evidence of an advantage to 1.5T in terms of either diagnosis or sensitivity to disease. In a large clinical trial involving patients with suspected multiple sclerosis, no difference in accuracy, sensitivity, or specificity was noted between 0.5 and 1.5T studies [1]. A similar design large-scale clinical trial was performed with patients referred for imaging of the knee [2]. Evaluation for anterior or posterior cruciate ligament and meniscal tears showed no advantage for the higher field strength in terms of accuracy and diagnosis.

In comparing 0.5 and 1.5T, the hypothesis still stands today as it did in 1996 “that applications that require very fast imaging, very high resolution imaging, or detection of very small image intensity changes *may* demonstrate diagnostic advantages for high magnetic field” [3]. It is important also to recall that some of the prominent arguments favoring 1.5T and above included techniques that are little used clinically today, such as spectroscopy, fiber tracking and functional MR. Also, making low-field much more viable are the many, significant technologic advances that occurred in the interval years. These are considered in the sections that follow. For a moment, however, let us consider the problem that we are confronted with, and that is the reality of physics in terms of signal-to-noise ratio (SNR) and contrast-to-noise ratio (CNR).

SNR increases linearly with field strength, with some assumptions. One is that receiver bandwidth is held constant. However, bandwidth for any particular scan sequence is usually increased at higher fields to account for chemical shift. When the pixel shift is held constant, then SNR scales with the square root of field strength (not linearly). CNR is a more complicated situation, in part due to the increase of T1 with field strength. Taking these factors into account, for T1-weighted scans the increase in CNR from 0.5 to 1.5T is in the range of 20%, while it can be more than 40% for scans with little T1 contribution.

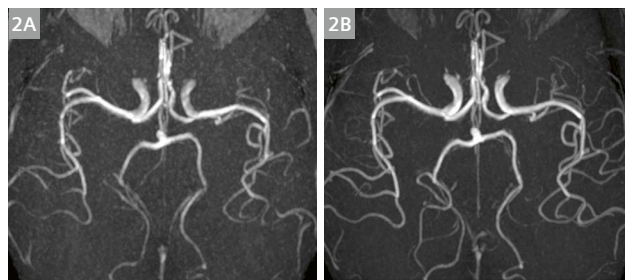
One caveat to the consideration of the data from the 1980s and 90s is that Time-of-Flight (TOF) MR Angiogra-

phy and contrast enhanced MRA were not evaluated. These techniques had not yet been invented. Thus, it remains a question – which is presently being answered – until next generation low-field units are further along in development how far interim software and hardware advances can close the gap in image quality for MRA between low and high field (Fig. 2).

What opportunities exist today for low-field MR?

The question is what opportunities exist for making MR accessible to a broader patient population, and/or more cost efficient [4]? The development of high field was pushed due to the promise of increased SNR and thus higher image quality. However, looking just at one area, and that is the spine, the march from 0.5 to 1.5 to 3T has not truly met one’s expectations. Chemical shift and CSF motion created problems, some of which still exist today, and slice thickness for routine scans only moved from 5 mm to 3–4 mm. Regardless, a modern low-field system is expected to achieve comparable image quality, and thus have sufficient SNR. Alternatively, for the installed site, the number of applications demanding thin section imaging need to be very low, to justify purchase of a system without such capabilities. It should be kept in mind however that thin section imaging in certain instances can be achieved with longer scan times.

Along the way – in the development of higher field units – new problems were encountered, due to – for example – SAR, patient safety, tissue susceptibility, and not to be forgotten, cost. In regard to the latter, the specifications and infrastructure requirements of MR-systems have grown substantially over the years, keeping MR an extremely expensive imaging modality, limiting patient access and utilization.



2 Time-of-flight MRA was not developed until relatively late for MR, and thus the question remained – answered with this figure – about the diagnostic potential at 0.55T. TOF MRA performs well, comparable to 1.5T, with, as anticipated, a slight reduction in SNR. Thick axial MIP reformats are presented from scans at (2A) 0.55T and (2B) 1.5T with voxel dimensions of $0.5 \times 0.5 \times 0.5 \text{ mm}^3$ in each instance and approximately the same scan time.

Today there is tremendous economic pressure on healthcare systems worldwide. Thus, the following questions seem worth revisiting. Is it possible to reduce the cost of the most expensive part of an MR system, the magnet, as well as the next most expensive part, the gradients, and still achieve excellent image quality? Is it thus possible to add new diagnostic value, by making MR more accessible both in developed countries and in less developed areas, as well as for niche applications (such as interventional MR)? Is there a missed opportunity in the road that clinical MR and the research community have taken since the advent of this technology in the 1980s?

Intrinsic advantages for low-field systems include shorter tissue T1 and longer T2* (allowing more time efficient scan acquisitions), reduced susceptibility effects, and reduced specific absorption rate (tissue heating). Reduced SAR lessens scan parameter constraints (flip angle, TR, number of slices) and diminishes heating of metal devices and implants. Low-field technology was last explored in depth in the 1980s, long before the development of many current acquisition and post-processing strategies, including spiral acquisition, parallel imaging, iterative reconstruction and most recently deep learning reconstruction.

A new look at low-field technology today is highly recommended, holding the potential for development of advanced, next generation MR systems with markedly lower cost yet excellent image quality. Such a development could lead to a wide range of new scanners, from basic systems destined for small clinics or developing nations to higher end niche systems including dedicated emergency room, intraoperative, and interventional units.

Magnet and receiver coil technology

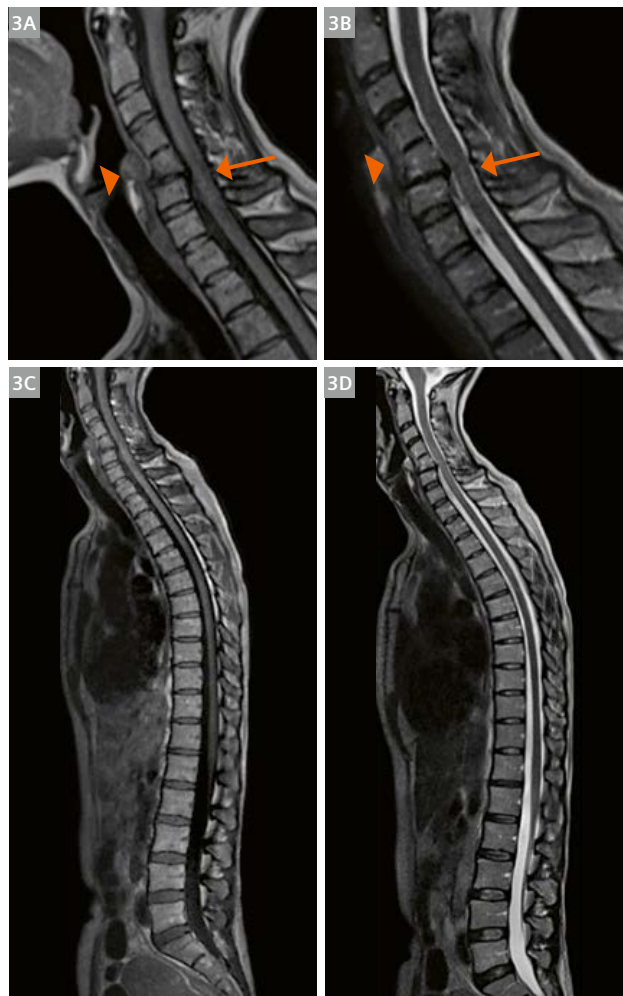
Bore size is an important consideration in design of an advanced, next generation low-field system. The early, whole body, superconducting MR clinical units had a 60 cm width bore, although the bore was even slightly smaller in several designs that were generally not successful.

The first wide bore (70 cm) unit, the MAGNETOM Espree (which operated at a field strength of 1.5T), was launched in 2004. This design at the time was highly innovative, and the unit subsequently dominated the sales market, largely due to patient comfort and the increasing weight of patients worldwide. Since that time, wide bore high field (3T) units have also become available. In terms of the design of a next generation low-field system, the comparatively small amount of superconducting wire needed makes viable, cost wise, ultra-wide-bore systems, with bore dimensions in the range of 80–90 cm.

A huge barrier, both from a practical point of view and cost, is the siting of a unit, for example in operating rooms, remote clinical sites, and developing world clinics. A zero boiloff magnet, with elimination of the quench pipe and a

markedly reduced foot print (including the 5 gauss line), are possible in the near future and offer great promise for dissemination of MR technology world-wide.

In terms of receiver coil technology, there have also been major advances since the 1980s that can be applied to next generation low-field systems. In the early years of MR, receiver coils were far from optimized, with for example head coils both larger in diameter and longer than needed. For body imaging, RF reception was

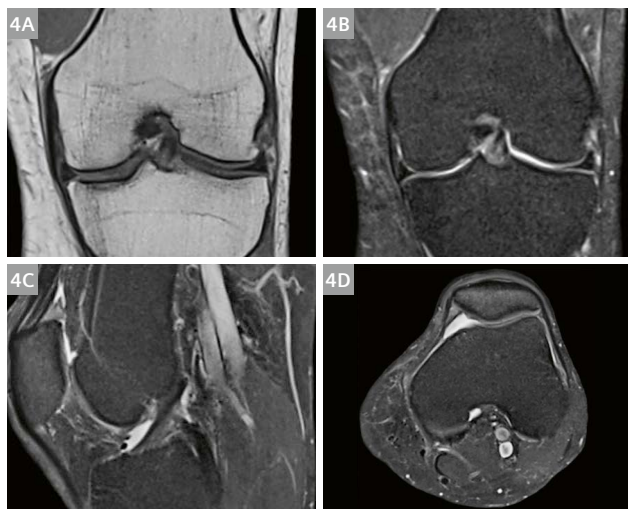


3 Sagittal (3A) T1- and (3B) T2-weighted 2D fast spin echo scans at 0.55T of the cervical spine. The slice thickness was 4 mm and 3 mm, respectively. Scan times were 3 minutes 10 seconds and 4 minutes 4 seconds. There is a mild retrolisthesis of C5 on C6. There is a disk-osteophyte complex at C5–6 with loss of disk space substance and mild endplate degenerative changes (arrow). The disk space at C4–5 is small (arrowhead), and given the appearance of the C4 and C5 vertebrae on the sagittal images, this likely represents a congenital block vertebral body (C4–5). The thoracic and lumbar spine that are displayed in the sagittal (3C) T1- and (3D) T2-weighted full spine images are essentially normal. The slice thickness in (3C) and (3D) was 4 mm. Scan times for the whole-spine scans were (3C) 9 minutes 30 seconds and (3D) 8 minutes 48 seconds.

performed using the body coil – placed far away from the patient and thus with relatively poor SNR. The advances we take for granted today – that have led to major improvements in SNR and paid into the capability for acquisition acceleration, such as multichannel, multielement coils, flexible coils, and specific contoured coils for body regions (for example the shoulder, knee, wrist, ankle, and neck) were in the 1980s and 1990s still decades away from development. Spine, musculoskeletal, and liver imaging at 0.55T will all benefit greatly from these technologic advances (Figs. 3–7).

Gradient performance

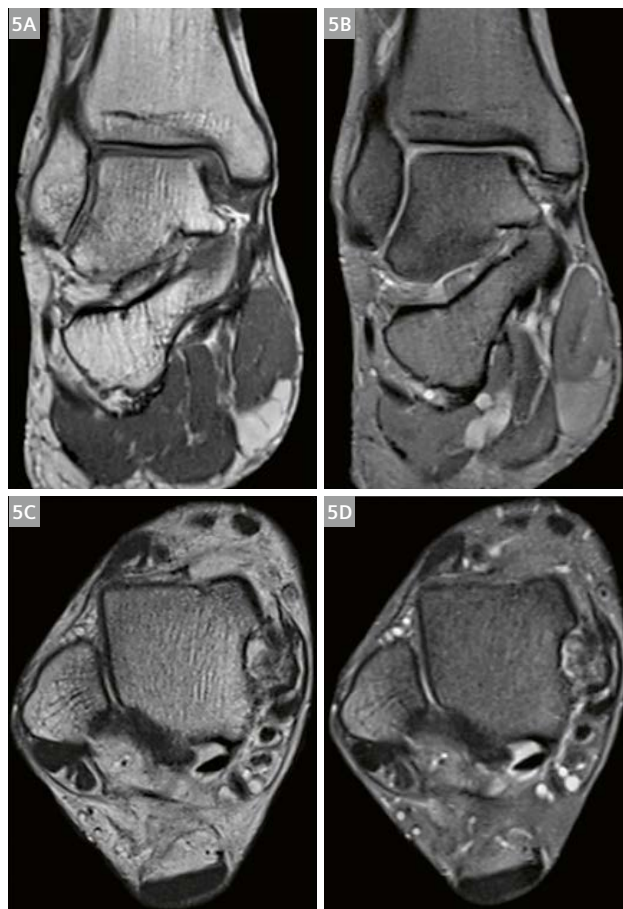
The gradient system is the second largest cost, following the magnet, for an MR unit. Over the years, there have been many advances regarding the magnetic field gradients, although today the slew-rate for whole body-systems is constrained not by technological limits but by physiology and specifically nerve stimulation. Research applications, for example high resolution DTI, however have primarily driven the quest for very high gradient amplitudes. There are cost issues here, due to manufacturing and design complexity, as well as increased power consumption and cooling requirements.



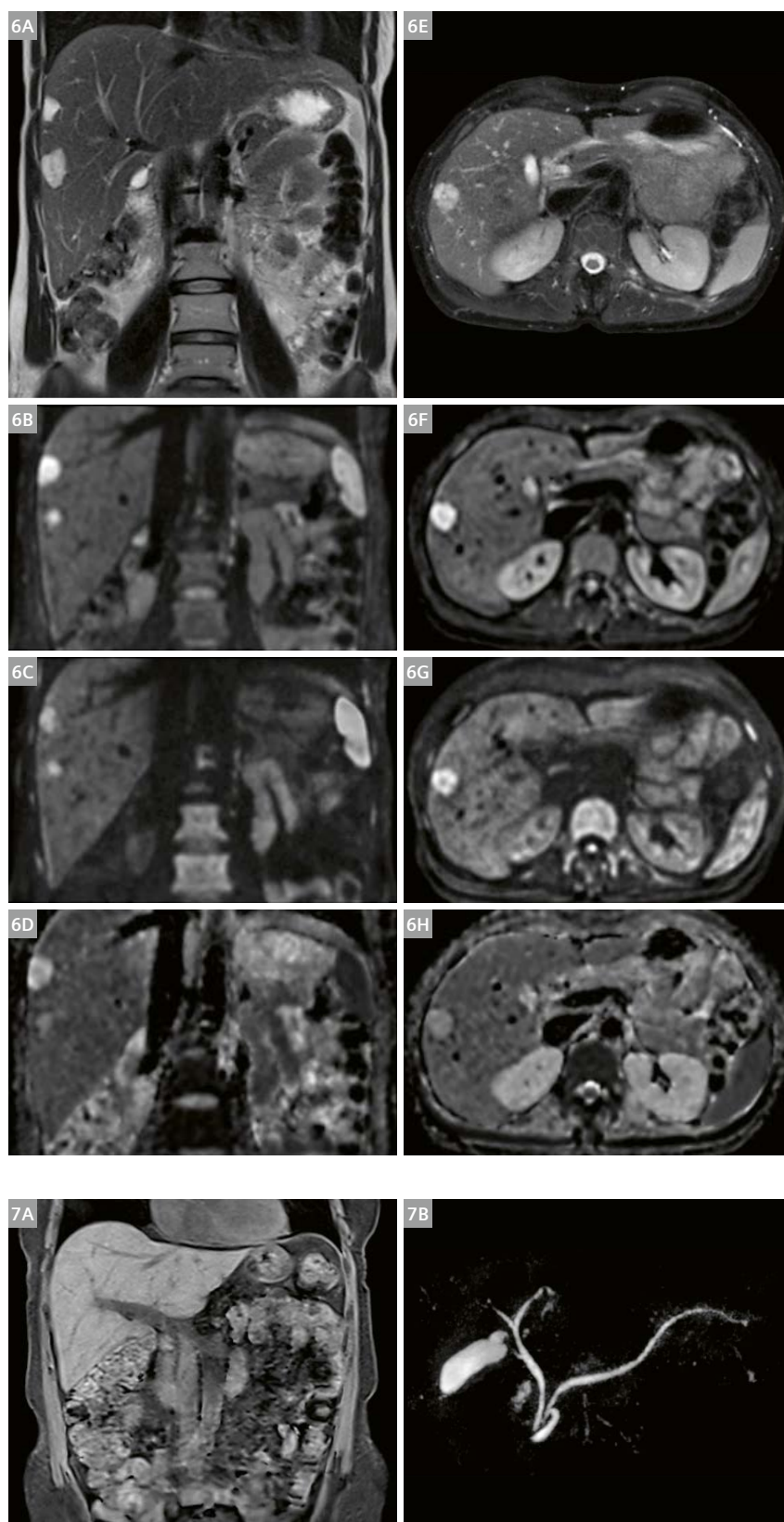
4 Coronal 2D fast spin echo (4A) T1-weighted images of the knee, and coronal, sagittal, and axial (4B, C, D) 2D proton density-weighted images with fat saturation, all images obtained at 0.55T in a normal volunteer. The slice thickness in each instance was 4 mm. Scan times were (4A) 4 minutes 4 seconds, (4B) 5 minutes 2 seconds, and (4C, D) 5 minutes 22 seconds, respectively.

However, much like cars, one does not always need a Ferrari, a BMW will do. One cannot always drive one's car at 200 kilometers an hour, and most Ferraris spend very little of their life doing such speeds. Thus, the question is, for MR, for daily, routine clinical use which techniques require peak amplitude of the gradients, how often are they used, and are there other ways to reach such requirements?

One of the techniques that drives the gradients the hardest is diffusion-weighted imaging (DWI). If one simply uses an older gradient system, with lower specifications, then the change required for high end DWI will be to



5 Coronal 2D fast spin echo proton density-weighted images of the upper ankle (5A) without and (5B) with fat saturation, obtained at 0.55T. Voxel dimensions were (5A) $0.5 \times 0.4 \times 3.0 \text{ mm}^3$ and (5B) $0.6 \times 0.5 \times 3.0 \text{ mm}^3$, with scan times of 3 minutes 47 seconds and 3 minutes 46 seconds. Axial 2D fast spin echo T2-weighted images of the upper ankle (5C) without and (5D) with fat saturation, obtained at 0.55T. Slice thickness of the T2-weighted images was 3 mm, scan time was 3 minutes 37 seconds and 3 minutes 19 seconds.



6 Coronal (**6A**) respiratory triggered 2D T2-weighted images of the abdomen, using a BLADE acquisition technique. Scan time was 2 minutes 26 seconds. Axial (**6E**) respiratory triggered 2D T2-weighted fat saturated images of the abdomen, using a BLADE fast spin echo acquisition. Scan time was 2 minutes 50 seconds. Images are presented from a normal volunteer at 0.55T and show two small liver hemangiomas with characteristic hyperintensity on T2w and hyperintensity on DWI and ADC. The $b = 50 \text{ s/mm}^2$ (**6B, F**) and $b = 800 \text{ s/mm}^2$ (**6C, G**) diffusion-weighted scans were obtained with single-shot echoplanar technique, the respective ADC-maps (**6D, H**) are also presented. Scan time for the coronal diffusion-weighted scans was 2 minutes 10 seconds, scan time for the axial diffusion-weighted scans was 3 minutes 26 seconds. The slice thickness was 6 mm in every instance.

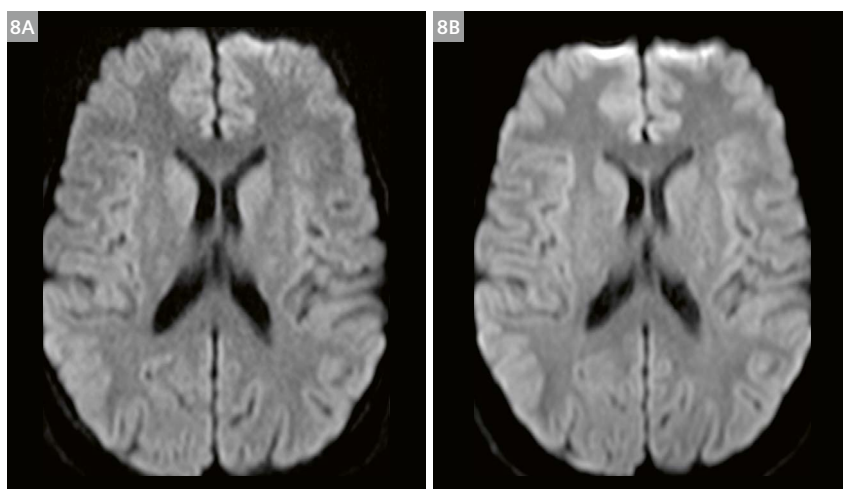
7 Coronal breath-hold 3D T1 VIBE Dixon water images (**7A**) of the abdomen with a slice thickness of 3 mm. The scan time was 19 seconds. MRCP (**7B**): MIP reformat from a respiratory-triggered 3D T2 SPACE acquisition, displaying the right and left hepatic duct, the common hepatic duct, the common bile duct, and the pancreatic duct. Voxel dimensions were $1.1 \times 1.0 \times 1.0 \text{ mm}^3$, with a scan time of 4 minutes 19 seconds (CS factor 10).

increase the TE on the order of 10–15 msec. At high field, this is actually a very substantial change. There, TE and echo spacing are kept as short as possible to minimize susceptibility and maximize SNR. However, at low-field, T2* decay and susceptibility are much less of an issue, with longer echo spacing acceptable and the SNR issue of longer TEs compensated with lower readout bandwidths (Fig. 8). This example illustrates the need to think outside the box for the design of low-field gradient systems. Balancing imaging parameters is an optimization problem with different boundary conditions at low-fields. By careful

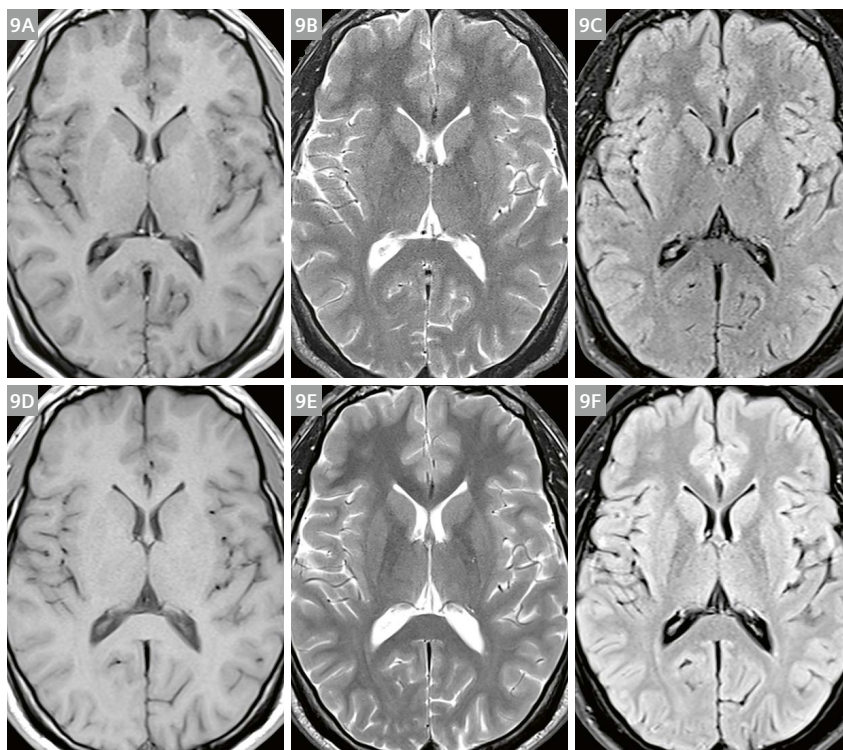
design, the potential disadvantages of a low cost gradient system can be mitigated with a non-traditional approach. High image quality can be achieved, with the lower cost of the magnet and gradients offering major advantages in terms of broadening access to MRI.

Image contrast

It is important to note that T1, T2, and T2* all change with magnetic field. Depending upon the specifics, this could be an advantage or a disadvantage for low-field (Fig. 9). T1 shortens by 1/3rd at low-field when compared to 1.5T,



8 2D single shot epi DWI ($b = 1000 \text{ s/mm}^2$) at (8A) 0.55T and (8B) 1.5T, acquired with the same slice thickness (5 mm) and pixel dimensions. Known problems at higher field can be seen, for example the image distortion anteriorly (due to susceptibility effects from the frontal sinus), mild image blurring, and slight image foreshortening – which are not present on the 0.55T image. Due to doubling of the number of averages, the scan time at 0.55T was about twice that at 1.5T.



9 2D TSE (9A, D) T1-weighted, (9B, E) T2-weighted, and (9C, F) FLAIR images of the brain at (9A–C) 0.55T and (9D–F) 1.5T. To be noted is the mildly improved T1 contrast at 0.55T, due to the increase in T1 with field strength. The slice thickness was 5 mm. Scan times ranged from approximately equal for the two fields to about twice, depending upon technique.

which is advantageous for T1-weighted scans. Other advantages, specifically for echo-planar and spiral acquisitions, include that T2 is longer by a 4th, and T2* longer by almost half. Low-field may have as well applications for lung imaging, where the situation is unique, with T2* prolonged more than 3-fold [5].

Spiral imaging

Improved signal sampling efficiency can be achieved at low-field due to the prolongation of T2*. Using a spiral out acquisition (as opposed to Cartesian sampling), balanced steady-state free precession and spin echo techniques can achieve nearly double the SNR [5]. The rationale for high field imaging was the gain in SNR, in theory (although with many caveats) being linear with the increase in field strength. A spiral out acquisition at 0.5T can offer a gain of two times in SNR, largely negating the three times higher (in theory) SNR at 1.5T.

Simultaneous multi-slice technique

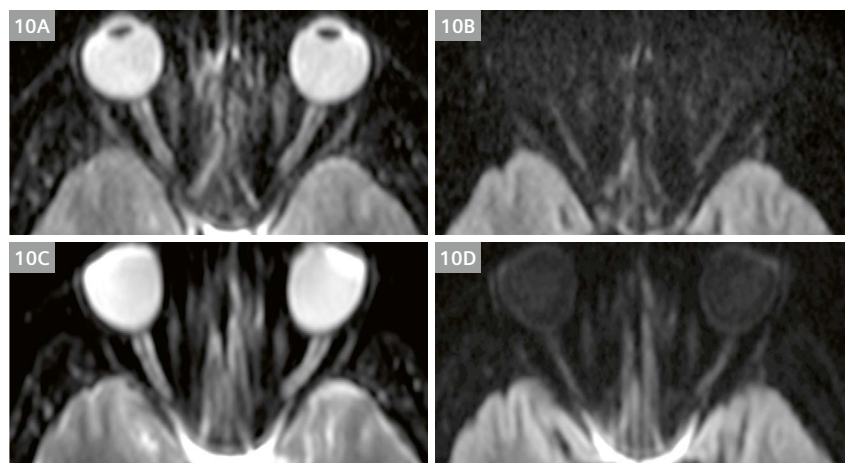
Simultaneous multi-slice (SMS) technique is not restricted to high field imaging, and is easily applied as well at low-

field. As shown in many clinical applications, SMS can be used to reduce scan time as well as to increase the number of acquired slices within a given scan time [6]. Its primary application at low-field will likely be to improve SNR, while maintaining scan time. This technique is easily applicable to both single shot EPI (for diffusion-weighted scans) and turbo spin echo technique (for T1-, T2-, and proton density-weighted scans).

Iterative denoising

Iterative denoising is a relatively new technique that can be applied to improve image quality for low SNR scans [7]. The technique could thus be of particular value for low-field scans. Iterative denoising can be applied to almost all routine 2D and 3D MR acquisitions. It has the potential to increase SNR by 25%, or alternatively to reduce scan time by 30% (while maintaining SNR).

A short explanation of iterative denoising follows. Complex-valued image data is exported prior to interpolation and magnitude reconstruction, together with additional information regarding image normalization, k-space filtering, and noise calibration used. This data



10 (10A, C) b-value 0 and (10B, D) 1000 s/mm² single shot EPI DWI scans at (10A, B) 0.55T and (10C, D) 1.5T of the orbit. The increased magnetic susceptibility at 1.5T leads to marked distortion of the globes, poor depiction of the optic nerves, and prominent susceptibility artifact from the sphenoid sinus. Sequence specifics were similar for the two field strengths, with signal averages doubled for 0.55T.



11 Coronal (11A) T2 TIRM and axial (11B) 2D BLADE fast spin echo proton density weighted images and axial (11C) 2D T2-weighted BLADE images of the thorax. All images were obtained with respiratory triggering in a healthy volunteer at 0.55T. Slice thickness was 6 mm. Scan times were 6 minutes 8 seconds, 7 minutes 22 seconds and 5 minutes 44 seconds, respectively.



is then iteratively denoised by thresholding – spatially adapted to the local noise level – using orthogonal wavelet transforms. The data is re-imported to the reconstruction pipeline and magnitude images calculated. An important point is that the process is automatic, with the algorithm adapting to changes in acquisition and scan conditions.

Deep learning reconstruction

Another highly promising, yet very new approach is to utilize deep neural networks either in the direct transformation of raw data into images or to optimize the quality of otherwise non-diagnostic images. Consider for the moment the simple example of a fast, low resolution scan acquired at low field. If a neural network is trained with high-resolution images – from either the same field strength or higher, the network can establish “neural connections” to associate features in the lower quality image with those in the higher quality image. After training on a few thousand images, the network can then apply its “knowledge” to improve the resolution of the images. This approach is commonly termed superresolution processing. Beyond such image optimization strategies, deep learning might also be beneficial to limit the impact of artifact patterns, such as streaking in radial imaging.

Image degradation due to susceptibility

The differing susceptibility of tissues causes, at their interface, both geometric distortion and artifactual areas of high and low signal intensity in MR images. Susceptibility is substantially less at low-field, being proportional to magnetic field strength. Prominent susceptibility artifacts, interfering with clinical diagnosis, are well known in the orbits, internal auditory canal, skull base, lungs, bowel, and close to metal implants. Considering this issue by itself, image quality will thus be substantially improved in these areas at low-field (Fig. 10). Lung imaging in particular will benefit, with MR of course offering potential clinical value over CT due to its soft tissue contrast and in particular the ability for spatially resolved assessment of lung function (Fig. 11). Recent clinical images from a 0.55T prototype show great potential for the imaging of parenchymal lung disease [5]. A particular advantage for MR in this application would also be the elimination of the high radiation dose otherwise necessary over a patient’s lifetime for the evaluation by CT of chronic diseases, in particular those that occur in the pediatric population, for example cystic fibrosis. The imaging of metal implants is another area expected to benefit greatly from low-field, due to less severe susceptibility artifacts.

Acoustic noise

The noise in MR, during scanning, comes from the gradient coils. If everything else is held constant, doubling the magnetic field increases the acoustic noise (which is measured on a logarithmic scale) by 6 dB(L) [8]. To put this in perspective, normal conversation is at 60 dB, a vacuum cleaner 75 dB, sounds above 85 dB harmful, and for a subway 90–95 dB. Many sound deadening designs for the gradients have been introduced over the history of MR, with all applicable regardless of field strength. In a comparison of a low-field and a 1.5T unit (performed in the early 2000s), acoustic noise ranged from 77 dB at low-field (with the lowest noise scan) to 98 dB at high field (with the highest noise sequence). With all else equal, and a scan that produces moderate noise, changing from a 1.5 to a 0.5T MR could reduce the noise of the gradients for example from that of a subway to that of a door bell.

Interventional MR

There are many special requirements for interventional MR. RF heating can be a concern, due to the use of biopsy needles and guidewires. Heating in MR generally scales with Larmor frequency, and thus the operating field strength. Low-field consequently offers major advantages over high field. This is particularly true for cardiac catheterization. A recent study at 0.55T demonstrated that heating, with a subset of currently available devices, did not represent a restriction, and specifically did not exceed 1°C during 2 minutes of continuous imaging [5]. For an interventional system, improved bore access (due to greater bore dimension) would also be a marked advantage.

The lower price of a low-field system (with the real cost including the system itself, installation, and service/cryogenics) would make much more practical dedicated installations for interventional work. Patient monitoring should be simpler, due to the lower field strength, with fewer problems caused by the magnetic field (for example with monitoring equipment) and the 5 gauss line much closer to the unit. The lower cost and ease of installation could lead to dedicated systems not previously possible in many departments, like what evolved historically with CT as well.

A substantially lower main magnetic field also reduces susceptibility artifacts, specifically the artifacts from catheters and needles. TrueFISP, the pulse sequence of choice for interventional guidance, also performs better at lower fields. SAR limits are less of a constraint, and other image artifacts (such as bending) are also less. Overall, low-field offers a major advantage when compared to higher fields such as 1.5T for interventional work.



Summary

Next generation low-field MR units will greatly benefit by the knowledge gained in system development over the last 35 years. High image quality is dependent on magnet homogeneity, fast gradients with minimal eddy currents, multichannel receiver coils and advanced image reconstruction (including compressed sensing), all achievable on a low cost, low-field system today. Developing in addition an advanced design ultrawide-bore magnet would offer unrivaled patient comfort and ease of patient monitoring, sedation, and interventions. The reduced acoustic noise inherent to low-field offers a further improvement in patient comfort, as well as that for associated personnel.

Low-field MRI is inherently more cost-effective due to reduced magnet, gradient, RF transmitter, and siting costs. Installation and infrastructure (weight, size) requirements are substantially reduced. The need for helium refills, and even the quench pipe, could be eliminated with an advanced magnet design, further reducing costs. These all have important implications for technology dissemination – both in developed economies and in underdeveloped areas [4], and access to care.

Not to be neglected are the specific imaging advantages that come with low-field. Lower susceptibility leads to improved sequence performance, as well as improved image quality in many anatomic areas. Lower SAR adds scan sequence flexibility and diminishes the difficulties with metal implants and interventional techniques. Advanced readout strategies with increased SNR, such as spiral imaging, are possible. SNR-efficient long readout strategies can be employed, due to reduced T_2^* , providing the benefit as well of reduced image distortion and blurring.

Newly designed, advanced generation low-field MR imaging systems will radically increase access to disease diagnosis and surveillance both in developed countries and worldwide. MR systems operating in the range of 0.5T were briefly evaluated in the mid-1980s, in the early days of MR. Considering the subsequent hardware and software developments over the interval 35 years, those units were quite primitive and did not reflect the image quality that can be achieved today. The potential impact of new, low cost, advanced generation MR imaging systems is extremely high. These will lead to further dissemination of health care – both in the G20 nations and in developing countries.

The low system cost, low installation cost, ease of maintenance, and ability to operate even with electrical power issues, combined with high image quality, all predict a bright future for this development.

References

- 1 Lee DH, Vellet AD, Eliasziw M, et al. MR imaging field strength: prospective evaluation of the diagnostic accuracy of MR for diagnosis of multiple sclerosis at 0.5 and 1.5 T. *Radiology*. 1995;194(1):257-62.
- 2 Vellet AD, Lee DH, Munk PL, et al. Anterior cruciate ligament tear: prospective evaluation of diagnostic accuracy of middle- and high-field-strength MR imaging at 1.5 and 0.5 T. *Radiology*. 1995;197(3):826-30.
- 3 Rutt BK, Lee DH. The impact of field strength on image quality in MRI. *J Magn Reson Imaging*. 1996;6(1):57-62.
- 4 Geethanath S, Vaughan JT, Jr. Accessible magnetic resonance imaging: A review. *J Magn Reson Imaging*. 2019;49(7):e65-e77.
- 5 Campbell-Washburn AE, Ramasawmy R, Restivo MC, et al. Opportunities in Interventional and Diagnostic Imaging by Using High-Performance Low-Field-Strength MRI. *Radiology*. 2019;293(2):384-93.
- 6 Runge VM, Richter JK, Heverhagen JT. Motion in Magnetic Resonance: New Paradigms for Improved Clinical Diagnosis. *Invest Radiol*. 2019;54(7):383-95.
- 7 Kang HJ, Lee JM, Ahn SJ, et al. Clinical Feasibility of Gadoteric Acid-Enhanced Isotropic High-Resolution 3-Dimensional Magnetic Resonance Cholangiography Using an Iterative Denoising Algorithm for Evaluation of the Biliary Anatomy of Living Liver Donors. *Invest Radiol*. 2019;54(2):103-9.
- 8 Moelker A, Wielopolski PA, Pattynama PM. Relationship between magnetic field strength and magnetic-resonance-related acoustic noise levels. *MAGMA*. 2003;16(1):52-5.

The figures are reproduced in part from Runge VM, Heverhagen JT, Advocating development of next generation, advanced design low-field MR systems, *Invest Radiol* 2020;55(12) with permission.



Contact

Val M. Runge, M.D.
Editor-in-Chief, Investigative Radiology
Department of Diagnostic,
Interventional and Pediatric Radiology
University Hospital of Bern, Inselspital
Bern
Switzerland
ValMurray.Runge@insel.ch

Brain MRI in an Emergency Department: Clinical Implementation and Experience in the First Year

Vincent Dunet, M.D.¹; Chantal Rohner, B.Sc.¹; David Rodrigues, B.Sc.¹; Jean-Baptiste Ledoux, B.Sc.^{1,2}; Tobias Kober, Ph.D.^{1,3}; Philippe Maeder, M.D.¹; Reto Meuli, M.D.¹; Sabine Schmidt, M.D.¹

¹Department of Diagnostic and Interventional Radiology, Lausanne University Hospital and University of Lausanne, Switzerland.

²Center for Biomedical Imaging (CIBM), Lausanne, Switzerland

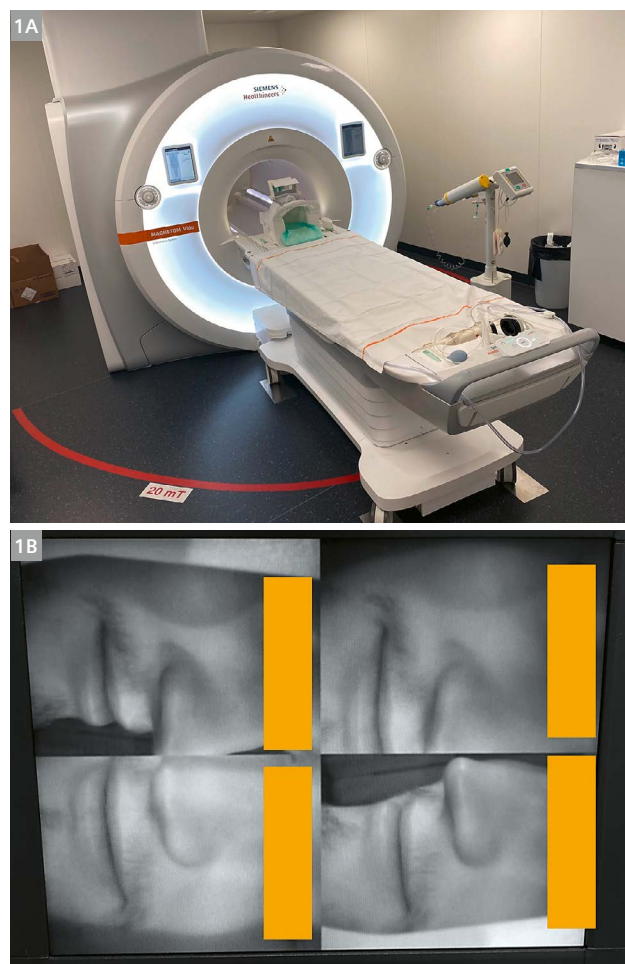
³Advanced Clinical Imaging Technology, Siemens Healthineers, Lausanne, Switzerland

Introduction

While computed tomography (CT) is generally used as a first-line investigation method in emergency departments, magnetic resonance imaging (MRI) is the reference method to accurately detect and characterize cerebral involvement and investigate subtle pathophysiological alterations in most brain diseases, including stroke, seizure, brain tumors, and infections.

Magnetic resonance (MR) investigation for patients referred to emergency departments remains challenging, as scanners are not always available 24/7 and patients are often unstable. Also, as longer acquisition times are needed compared to CT imaging, a strict selection of indications that could benefit from MRI without unnecessarily prolonging the patient workup is mandatory in order to optimize time-to-treatment.

A 3T MAGNETOM Vida scanner (Siemens Healthcare, Erlangen, Germany) was installed in the Emergency Radiological Unit of the Department of Diagnostic and Interventional Radiology of the University Hospital of Lausanne at the end of December 2017 (Fig. 1). To date, this is the first MR scanner located directly within an emergency department in Switzerland. We present brain MR workflow implementation and current brain MR guidelines in the emergency setting. We also report on the activity during the first year of use and results after the first 1,000 brain MR cases.



1 3T MAGNETOM Vida scanner and cameras

The 3T MAGNETOM Vida scanner (1A) was installed in the Emergency Radiological Unit and was equipped with three cameras: one at the top of the bore and four mounted into the bore (1B) to allow monitoring of patients' face and motion on screens in the control room.

MR workflow implementation

MR activity started on January 1, 2018, with 12-hour daily availability until the end of March, followed by 24/7 availability from April 2018. On May 1, 2018 (week 18), we also started using MRI in the 24/7 acute stroke workflow. Emergency department collaborators, including nurses and physicians, were given MR safety information and guidelines on implementing brain MRI both for daily emergency practice as well as for the acute stroke workflow. We also developed a harmonized multi-disciplinary list of indications.

From the beginning, our MR activity was not limited to brain imaging, but also included body imaging for urgent indications for which MRI remains the reference standard, such as the search for bile duct stones.

MR safety

The use of MRI in an emergency setting is a challenge for patient safety and management, so it was necessary to prepare the Emergency Department and Neurology teams. From December 2017 to March 2018, 100 nurses and physicians were given 20 teaching sessions that covered MR setup, safety rules in the MR environment, and MR safety checklists (one for employees, one for patients).

Teaching also included stroke-like workflow simulations, with a volunteer simulating a stroke complicated by an acute seizure that occurred in the MR scanner. Each simulation involved a neuroradiologist, a neurologist, a physician from the Emergency Department, two MR technologists, and two nurses, all blinded for volunteer behavior. Each step was timed, and the availability of materials

and respect of MR safety rules were checked by a separate team consisting of one neuroradiologist, one MR technologist, one neurologist, and one physician from the Emergency Department. A debriefing meeting for all participants followed. A second simulation was then conducted to ensure that performance had improved, before making MR available for acute stroke 24/7.

To ensure patient safety during MRI acquisition, EKG, arterial blood pressure, respiratory rate, and oxygen saturation index were continuously monitored on repetition screens in the control room. Furthermore, position, and patients' faces were monitored via dedicated cameras inside the tunnel (Fig. 1).

MR indications and contraindications

A complete switch from CT imaging to MRI is not feasible in an Emergency Department due to the difference in acquisition time, as well as frequent hemodynamic instability and restlessness of admitted patients. It is therefore crucial to determine indications and contraindications in patients that could benefit from a brain MRI.

After multi-disciplinary meetings with the responsible physicians at the Emergency Department (emergency and intensive care physicians, anesthesiologists, neurologists, neurosurgeons), we defined a list of indications for access to MRI within reasonable delay times (Table 1). We also set MR contraindications, including high level of restlessness, hemodynamic or respiratory instability, vomiting, severe claustrophobia, and implanted devices (pacemaker, neurostimulator, cochlear implant, or any fixed head or neck device).

Brain MRI indications and delay	
MRI within 30 min	MRI within 3 h
Acute stroke ≤8h with potential IVT or EVT Acute stroke >8h with potential late EVT	Acute coma Meningo-encephalitis Pituitary apoplexia before emergency surgery Brain tumor before emergency decompressive surgery
MRI within 6 h	No indication for MRI within 6 h
TIA or acute stroke without IVT or EVT Isolated acute vertigo without any peripheral cause Seizure and refractory status epilepticus Multiple sclerosis and RBON Intracranial hypotension	Any MRI contraindication (CT) Meningitis without focal deficit (CT) Initial workup of an extracerebral tumor without symptoms Acute hemorrhage (angio-CT) Isolated acute headache (angio-CT) Acute brain trauma (CT) Brain tumor with no need for emergency surgery

Table 1: Summary indications for emergency brain MRI and delay.

Abbreviations:

EVT: endovascular thrombectomy

IVT: intravenous thrombolysis

RBON: retrobulbar optical neuritis

TIA: transient ischemic attack



Some patients may have implanted devices but are not able to communicate in emergency situations, for example because of aphasia or cognition problems, so it was decided to perform a chest X-ray before MRI for any unresponsive patient admitted to the Emergency Department without recent documentation in our picture archiving and communication system. This is important especially for patients referred within the context of the acute stroke workflow. The initial evaluation by neurologists includes filling in the patient's safety checklist to decide between CT and MR imaging.

MR protocols

For most emergency cases, MRI is performed with a 64-channel array coil using standard MR protocols, as set up for outpatients; but MR acquisitions in cases of suspected stroke deserve special attention.

Although the choice of CT imaging or MRI does not influence the outcome of patients with acute stroke due to large vessel occlusion [1], MRI is superior to CT imaging for the diagnosis of small ischemic lesions and stroke mimickers [2–4]. However, the use of MRI delays patient management due to longer patient positioning and acquisition time [1], so MR protocols must be optimized. Fast MR sequences reduce acquisition time and the potential

impact of patient motion. It is, however, important not to inconsistently reduce the number of MR sequences, and consequently image quality, in order to take advantage of using MRI rather than CT imaging. Given that “time is brain” in a suspected acute stroke, the implementation of MRI needs cautious protocol optimization in order to reduce the “time to therapy”. Therapy being intravenous thrombolysis (IVT) and/or endovascular thrombectomy (EVT).

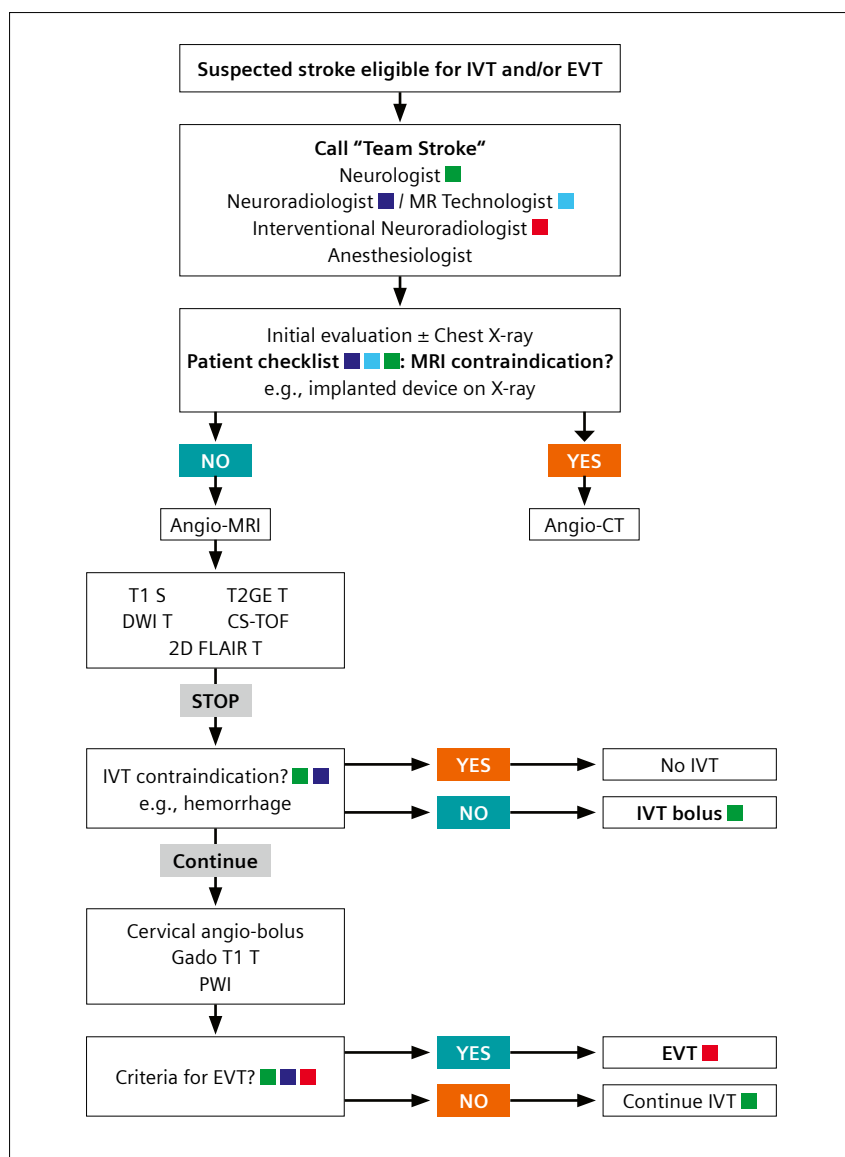
Starting with MR protocols previously used in our institution, we optimized our MR stroke protocol by adapting the number and duration of sequences while keeping optimal spatial resolution (Table 2). The choice following multi-disciplinary discussions was for the “short protocol with 3 mm thick slices and CS-TOF”, which represents the best compromise between high image quality, resolution and sequence duration. This protocol was designed for all MRIs performed for suspected acute stroke that could potentially benefit from IVT and/or EVT. Neither the ultra-short protocol nor the short protocol with 5 mm thick slices were chosen because arterial intracranial TOF is necessary for EVT planification, and because thin slices are more suitable for the detection of small infarcts, respectively. Figure 2 summarizes the current workflow for any suspected acute stroke case that may benefit from IVT and EVT.

Sequences	Full protocol	Protocol without suspicion of cervical dissection	Short protocol 3 mm thick slices with CS-TOF	Short protocol 5 mm thick slices with CS-TOF	Ultra-short protocol 3 mm thick slices without TOF
T1_fl2d_sag	1'10	1'10	1'10	0'53	1'10
ep2d_diff_AVC*	1'54	1'54	1'54	1'46	1'54
T2_tse_FLAIR_tra	2'24	2'24	2'24	1'47	2'24
T2_gre_tra_hemo	2'08	2'08	2'08	1'24	2'08
Tof_fl3d_tra_art	6'12	6'12	—	—	—
CS_Tof_fl3d_tra_art	—	—	3'06	3'06	—
T1_space_cor_spair	4'53	—	—	—	—
Angio_fl3d_cor_pre	0'23	0'23	0'23	0'23	0'23
Care_bolus_cor	1'30	1'30	1'30	1'30	1'30
Angio_fl3d_cor_post	0'23	0'23	0'23	0'23	0'23
T1_fl2d_tra	1'05	1'05	1'05	1'05	1'05
ep2d_perf_p3HR	1'45	1'45	1'45	1'45	1'45
Total duration	23'47	18'54	15'48	14'02	12'42

Table 2: Optimization of brain MRI protocols for acute stroke evaluation.

Abbreviations: CS, Compressed Sensing; FLAIR, fluid attenuated inversion recovery; TOF, time-of-flight.

* Diffusion-weighted imaging is acquired using Simultaneous Multi-Slice acceleration technology.



2 Acute stroke workflow

Abbreviations:

CS: compressed sensing

DWI: diffusion-weighted imaging

EVT: endovascular thrombectomy

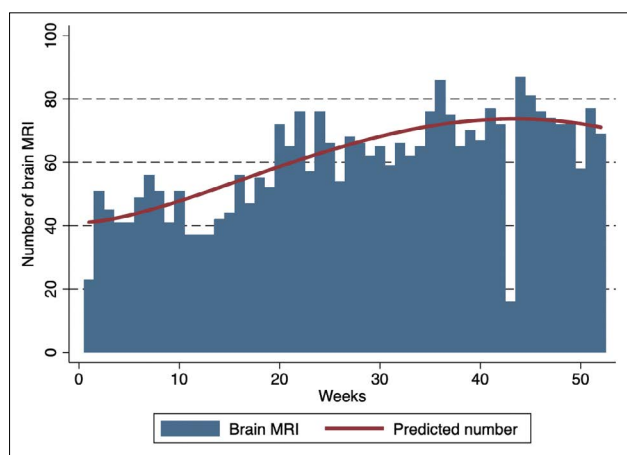
IVT: intravenous thrombolysis

PWI: perfusion weighted imaging

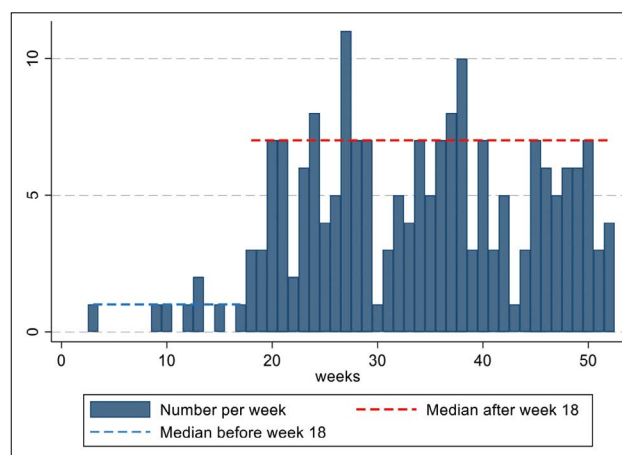
TOF: time-of-flight

Color points represent practitioners involved in the step:

- green for neurologist
- navy blue for neuroradiologist
- cyan for MR technologist
- red for interventional neuroradiologist
- Multiple points are displayed when a multidisciplinary decision is needed.



3 Emergency MRI activity over the first year.



4 Number of brain MRI scans recorded in the Acute Stroke Registry and Analysis of Lausanne.

Experience in the first year

Activity in the first year

Overall, 4,127 MRI exams were performed during the first year. Of these, 3,107 (75%) were brain MRIs. The weekly median number of brain MRIs was 66 (Interquartile range: 55–75, min-max range 16–87). This increased during the first few months from 45 (Interquartile range: 41–51, min-max range 23–56) before week 18, to 70 in the following months (Interquartile range: 65–76, min-max range 16–87). A plateau of 74 was reached at week 35 (i.e. last week of August, median number of brain MRI: 74 per week, interquartile range: 70–77, min-max range 16–87, Fig. 3). This corresponds to a prediction of up to 5,000 MRI scans per year with 24/7 MR scanner availability.

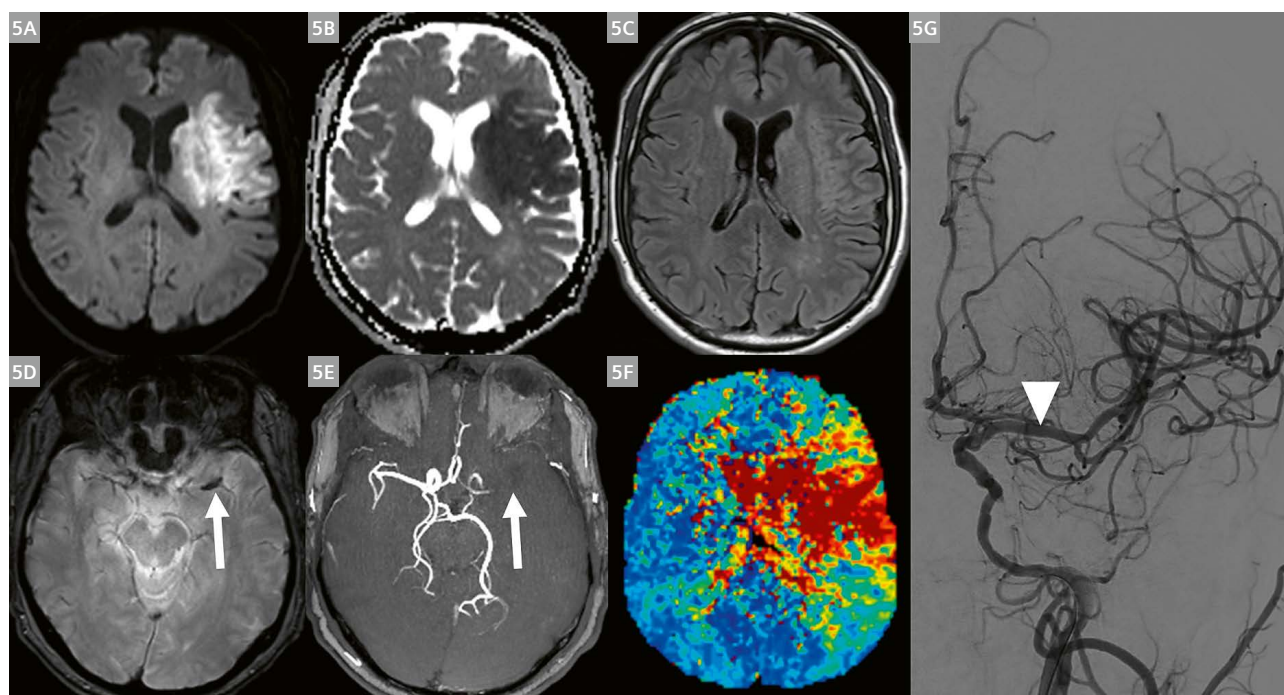
According to the Acute Stroke Registry and Analysis of Lausanne (ASTRAL), the number of patients who underwent a brain MRI at the acute phase of a stroke increased from a median of 1 case per week before week 18 (when the 24/7 acute stroke MRI workflow began) to 7 patients per week thereafter (Fig. 4).

The first 1,000 brain MR examinations: indications, protocols, and results

During the first five months, a total of 1,397 MR examinations were performed, including 1,000 brain MRIs. Of those 1,000 patients, 461 were female and 539 were male, with a median age of 57.2 years (95% interval 42–75 years; range 0–95 years).

Out of these first 1,000 brain MR examinations, 564 were for suspected stroke, 111 for other suspected vascular disease, 51 for seizure, 49 for suspected infection, 177 for known or suspected tumors, 31 for new psychological symptoms, and 17 miscellaneous. A total of 676 included the arterial TOF sequence, and 356 included both the arterial TOF and the cervical angio-bolus sequences.

Overall, 380 brain MRI scans (38%) were determined to be normal. The pathological results were stroke (Fig. 5) in 253 patients (25.3%), other vascular diseases (e.g., aneurysm, venous thrombosis) in 85, acute infection in 60, cerebral tumors in 173, and other miscellaneous diagnoses in 47 patients. MRI acquisition had to be stopped due to intractable nervousness in just two cases. We recorded no major adverse events due to MRI, or side effects after intravenous gadolinium contrast media injection.



5 Acute stroke on MRI

An early acute stroke of the left middle cerebral artery (MCA) is seen as a bright area on the diffusion-weighted image (5A); as an area with low ADC value (5B); and as a faint hyperintense area on FLAIR (5C). The thrombus located within the left MCA appears dark on the T2 gradient echo image (5D, arrow) and CS-TOF confirmed vessel occlusion (5E). On perfusion-weighted images, the T_{\max} map (5F) shows a large area of penumbra surrounding the infarct. The patient consequently underwent intravenous thrombolysis followed by endovascular thrombectomy, with subsequent complete recanalization of the left MCA as seen on end-procedure digital subtraction angiography (5G, arrow head).



Discussion

The clinical integration of an MR scanner into an emergency department is feasible. It requires prior teaching of adequate safety rules, multidisciplinary meetings to define the exact indications, and optimization of MR acquisition protocols. When these preliminary conditions are fulfilled, as was achieved in our institution, MRI use could quickly increase up to 5,000 cases per year.

While stroke is the top diagnosis in pathological examinations, we found that 38% of patients admitted to the emergency department with an indication for brain MRI had a normal result. Although the impact on the time of patient discharge from hospital has not yet been assessed, the use of MR in an emergency department could shorten the duration of hospitalization for patients with a normal brain or other MRI.

The true conversion rate from CT imaging to MR examinations should also be evaluated in our institution and in others. Unlike other countries and cities in Switzerland, our department has centralized management of all radiological emergency prescriptions, and a single general radiologist who decides on the imaging modality based on our guidelines. MR activity and conversion from CT imaging to MRI might therefore differ if modalities are managed by multiple practitioners, as is the case in Germany.

References

- 1 Menjot de Champfleury N, Saver JL, Goyal M, Jahan R, Diener HC, Bonafe A, Levy EI, Pereira VM, Cognard C, Yavagal DR, Albers GW. Efficacy of Stent-Retriever Thrombectomy in Magnetic Resonance Imaging Versus Computed Tomographic Perfusion-Selected Patients in SWIFT PRIME Trial (Solitaire FR With the Intention for Thrombectomy as Primary Endovascular Treatment for Acute Ischemic Stroke). *Stroke*. 2017;48(6):1560-1566. doi:10.1161/STROKEAHA.117.016669
- 2 Biesbroek JM, Niesten JM, Dankbaar JW, Biessels GJ, Velthuis BK, Reitsma JB, van der Schaaf IC. Diagnostic accuracy of CT perfusion imaging for detecting acute ischemic stroke: a systematic review and meta-analysis. *Cerebrovasc Dis*. 2013;35(6):493-501. doi:10.1159/000350200
- 3 Brazzelli M, Sandercock PA, Chappell FM, Celani MG, Righetti E, Arestis N, Wardlaw JM, Deeks JJ. Magnetic resonance imaging versus computed tomography for detection of acute vascular lesions in patients presenting with stroke symptoms. *Cochrane Database Syst Rev*. 2009;4:CD007424. doi:10.1002/14651858.CD007424.pub2
- 4 Schaefer PW, Barak ER, Kamalian S, Gharai LR, Schwamm L, Gonzalez RG, Lev MH. Quantitative assessment of core/penumbra mismatch in acute stroke: CT and MR perfusion imaging are strongly correlated when sufficient brain volume is imaged. *Stroke*. 2008;39(11):2986-2992. doi:10.1161/STROKEAHA.107.513358



Contact

Dr. Vincent Dunet
Department of Diagnostic and
Interventional Radiology
Lausanne University Hospital
Rue du Bugnon 46
CH-1011 Lausanne
Switzerland
Vincent.Dunet@chuv.ch

Iterative Denoising Applied to 3D SPACE CAIPIRINHA: A New Approach to Accelerate 3D Brain Examination in Clinical Routine

Alexis Vaussy¹; Michael Eliezer²; Nicolas Menjot de Champfleury³; Emmanuelle Le Bars³; Thien Huong Nguyen⁴; Christophe Habas⁴; Alto Stemmer⁵; Thomas Trolen¹

¹Siemens Healthineers, Saint-Denis, France

²Department of Neuroradiology, Lariboisière University Hospital, Paris, France

³Department of Neuroradiology, Hôpital Gui de Chauliac, Montpellier University Medical Center, Montpellier, France

⁴Radiodiagnostic and Medical Imaging, Quinze-Vingts National Ophthalmology Hospital, Paris, France

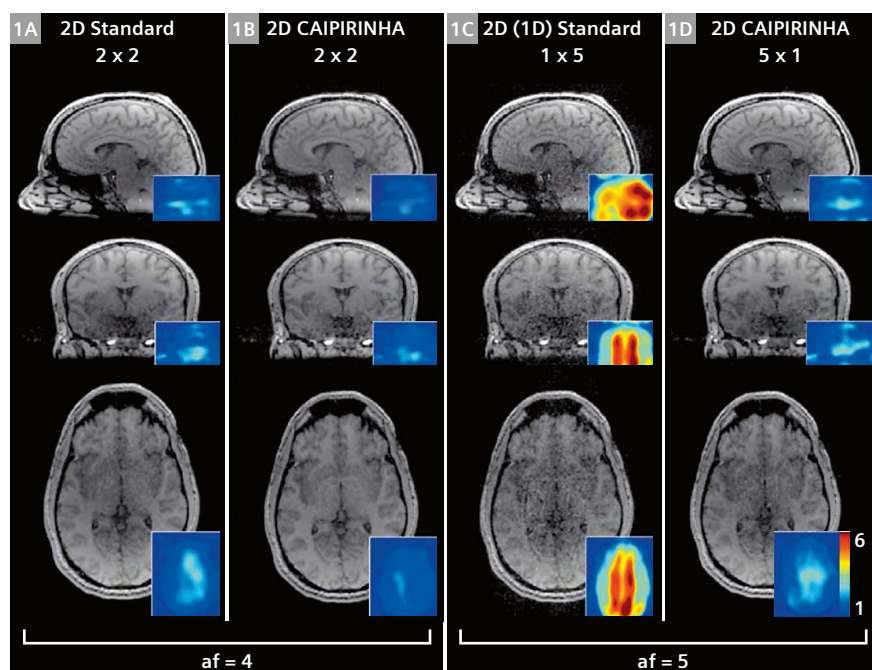
⁵Siemens Healthineers, Erlangen, Germany

Introduction

Magnetic Resonance Imaging (MRI) is an inherently slow imaging modality, since it acquires multi-dimensional k -space data through 1-dimensional (1D) free induction decay or echo signals. This can limit the use of long acquisition time sequences in clinical practice, especially for high-resolution or dynamic imaging. For that reason, one of the main aims over the past three decades has been to focus research and development activities on various acceleration techniques. Parallel imaging (PI) is the most commonly used acceleration technique. PI allows to reduce the number of k -space lines needed and to reconstruct the final images without aliasing artifacts. Parallel imaging has

emerged in the late 90's with SENSE [1] and GRAPPA [2] techniques. These pioneering works demonstrated that spatial diversity information from coil sensitivity maps have additional information that can be exploited to speed-up signal acquisition. The data redundancy in Fourier encoding of 2D or 3D spaces can be used to reduce the required sampling rate, in other words, without the need to satisfy Nyquist sampling criteria to avoid aliasing artifacts.

The penalty for acquiring fewer signals is a loss of signal-to-noise ratio (SNR) in the final image by a factor of the square root of the acceleration factor (\sqrt{R}) due to reduced signal averaging [3]. Additionally, PI reconstruc-



1 In vivo 3D FLASH brain imaging using different acceleration schemes with a 20-channels Head&Neck coil: (1A) Standard 2D-GRAPPA 2 x 2. (1B) 2D-CAIPIRINHA 2 x 2. (1C) Standard 5 x 1. (1D) 2D-CAIPIRINHA 1 x 5. Displayed are central slices in the sagittal, coronal, and axial view. In addition, the corresponding GRAPPA g-factor maps are shown. Reproduced with permission from [6].



tions result in spatially varying noise amplification in the final images, characterized by the so-called *g*-factor, which depends on the specific geometry of the radiofrequency (RF) coil array used for signal reception.

More recently, Controlled Aliasing in Parallel Imaging Results in Higher Acceleration (CAIPIRINHA) was first introduced for 2D multi-slice imaging [4] and then for volumetric 3D imaging (known as 2D CAIPIRINHA) [5]. This concept in PI modifies the appearance of aliasing artifacts during data acquisition in order to improve the subsequent PI reconstruction procedure by reducing the *g*-factor for a certain coil geometry and a certain imaging protocol. CAIPIRINHA applied to 3D imaging has been shown to be superior to more standard 2D SENSE/GRAPPA schemes in terms of signal loss and image quality [6], especially in the central part of the field of view (Fig. 1). This acceleration technique has been successfully implemented as a product solution unique to Siemens Healthineers, initially in the FLASH 3D Volumetric Interpolated Breath-hold Examination (f13d_vibe) sequence for body applications, and later in the Sampling Perfection with Application-optimized Contrasts using a different flip angle Evolutions (SPACE) sequence for spin-echo based 3D acquisitions throughout the human body.

The common theme in these approaches is that the data redundancy can be exploited to reduce the required sampling rate. Since redundant data can be compactly represented in some transform domains, it is also closely related to the concept of ‘*sparsity*’. Ever since the introduction of the Compressed Sensing (CS) theory [7] and the first demonstration of CS MRI by Lustig et al. [8], CS has become the essential tool in modern MR imaging research by exploiting image sparsity to reduce scan time and/or improve image quality.

The three key components of CS are

- the incoherent subsampling of the Fourier space,
- the transformation of the image into a sparse representation, e.g., Wavelet transformation, and
- the non-linear iterative reconstruction to balance between enforcing sparsity and ensuring data consistency.

A comprehensive overview of the CS theory, applications, and limitations can be found in [9] and [10]. CS was first integrated into product sequences on MR systems from Siemens Healthineers for cardiac cine applications, exploiting the 2D+t data redundancy of the beating heart, and for post-gadolinium 3D+t liver dynamics by the aim of Golden-Angle Radial Sparse Parallel (GRASP) MRI acquisition. CS was then integrated into additional sparse applications such as Time-Of-Flight MR angiography

(CS TOF), MR cholangiopancreatography using 3D SPACE readout (CS SPACE), and Slice Encoding for Metal Artifact Correction (CS SEMAC) for musculoskeletal applications in the presence of medical implants.¹

Limitation of CS for non-sparse images

MRI is all about tradeoffs. The time available for acquiring the data for an MR image can be deployed in three quite different strategies: SNR, contrast, and spatial resolution. Due to their inherently low sparsity, some applications offer little acceleration potential with CS, these include 2D multi-slice imaging or static morphological 3D sequences where high spatial resolution is essential to analyze fine structures.

For 2D multi-slice imaging, the Simultaneous Multi-Slice (SMS) acceleration technique has been implemented and has already shown great potential to drastically reduce scan time without compromising image quality in MRI diffusion [11]. SMS consists of the simultaneous excitation of multiple slices by means of multiband RF pulses, combined with a slice-GRAPPA reconstruction algorithm to disentangle the simultaneously excited slices prior to standard 2D reconstruction. While this approach is best suited for 2D sequences, it can also be adapted to 3D multi-slab applications. However, it is not applicable for single-slab 3D static morphological scans.

Another potential pitfall of CS for 3D static morphological imaging is the presence of ‘not so common’ artifacts such as image blurring and a ‘global ringing’ similar in appearance to motion ghosting. These can have deleterious effects even at a two-fold acceleration [12] and have been described for MR neuroimaging [13]. While the presence of artifacts in any accelerated image is an expected phenomenon, the unfamiliar and unpredictable nature of these artifacts means that radiologists or technologists may not be able to troubleshoot or even recognize them which can limit the usage of modern CS applications in clinical routine. For this reason, recent studies performed on 3D static morphological neuroimaging usually do not exceed three to four acceleration rates [14, 15].

In this work, we propose to investigate the use of high acceleration factors using standard CAIPIRINHA acceleration for cartesian trajectories, in combination with a modern iterative denoising (ID) reconstruction algorithm. Applied to the 3D SPACE sequence for neurological imaging, we demonstrate that capturing the high frequencies of the Fourier space helps to maintain image sharpness, while the denoising reconstruction maintains a high SNR in the final 3D volumes.

¹The MRI restrictions (if any) of the metal implant must be considered prior to patient undergoing MRI exam. MR imaging of patients with metallic implants brings specific risks. However, certain implants are approved by the governing regulatory bodies to be MR conditionally safe. For such implants, the previously mentioned warning may not be applicable. Please contact the implant manufacturer for the specific conditional information. The conditions for MR safety are the responsibility of the implant manufacturer, not of Siemens Healthineers.



Optimized SPACE CAIPIRINHA and Iterative Denoising

Turbo Spin Echo (TSE) based sequences are the workhorse of modern neuro imaging. While 2D TSE is commonly used in clinical routine for its acquisition speed and robustness, 3D TSE using variable refocusing pulses [16], known as SPACE, tends to replace 2D TSE imaging in clinical practice. Some imperfections have however been reported that limit its widespread use as a clinical standard in neuroimaging. These include the following:

- The increased scan time and its inherent sensitivity to patient motion.
- The resulting contrast that can be less marked than for 2D TSE due to the hybrid T1/T2 weighting in the readout train.
- The natural black-blood effect of TSE that can be limited for slow or turbulent flow using a thick excitation slab or non-selective RF-pulses.
- The presence of 'FID' artifacts caused by the variable refocusing pulses that create stimulated echoes along the readout.

Contrast optimization

T2 preparation applied to T2w SPACE FLAIR and DIR contrasts

3D Fluid-Attenuated Inversion Recovery (FLAIR) and Double Inversion Recovery (DIR) are well-established sequences in neuro examinations to improve brain lesion conspicuity. FLAIR uses an inversion preparation pulse combined with a long inversion time (TI) to suppress Cerebro-Spinal Fluid (CSF) magnetization. DIR uses two inversion pulses for suppressing white matter (WM) and CSF. However, it remains challenging to acquire whole-brain high-resolution 3D FLAIR/DIR in a clinically compatible scan time without compromising image quality, contrast, or SNR.

It is well established that 3T field strength is highly desirable over conventional 1.5T to improve lesion conspicuity in clinical neuroimaging. However, the consequence of a higher field strength is the lengthening of the T1 relaxation time of gray and white matter (GM and WM), while the T1 of CSF remains unchanged. As a result, the longitudinal magnetization recovery of GM and WM for a fixed repetition time is progressively reduced at higher field strengths, decreasing the lesion detectability due to increased T1 weighting. Furthermore, this incomplete magnetization recovery also compromises the theoretical SNR gain of a higher field strength.

An elegant way of addressing this issue is to use a T2 preparation module prior to the inversion pulse to mitigate the unwanted T1 weighting [17]. This preparation includes a 90° excitation RF pulse followed by a variable number

of 180° refocusing pulses and finally a -90° flip-back RF pulse [18]. Specific timing is required so that the transversal magnetization of GM and WM (with comparatively short T2 relaxation times) significantly decays while CSF transversal magnetization is nearly unaffected before the flip-back pulse. After inversion, CSF experiences an inversion recovery (as without T2 preparation module), while GM and WM experience a saturation recovery. This results in more complete recovery of GM and WM during the T1 period and hence less unwanted T1-weighting than without a T2 preparation module.

DANTE preparation applied to T1w SPACE

The 3D T1w SPACE sequence has been increasingly used in clinical routine since the development of the variable flip angle technique with non-selective refocusing pulses and short echo spacing [19]. 3D T1w SPACE is now proposed as an alternative to the 3D Magnetization Prepared Rapid Gradient Echo (MPRAGE) sequence due to its inherent reduction of artifacts from static field inhomogeneity and its better sensitivity for the detection of brain lesions or metastases. The advantages of 3D T1w SPACE over 3D T1w MPRAGE have been demonstrated for several applications, such as brain metastases [20] and multiple sclerosis [21] indications. The use of long echo train length (ETL) is mandatory to achieve a scan time compatible with clinical routine and allows for more effective flow suppression without compromising image quality and sensitivity. Long ETL also have the advantage to provide inherent black-blood effect.

However, residual slow blood signal may persist and mimic atherosclerotic plaque or vessel wall disease. This issue is especially present after gadolinium contrast agent injection, as the blood suppression efficiency is reduced by the shortened T1. Several techniques have been proposed to reduce residual blood flow effects, such as DIR preparations for cardiac imaging and a flow sensitive gradient technique called Motion Sensitized Driven Equilibrium (MSDE) for neuro imaging.

The use of DIR preparation provides an effective blood signal suppression but is limited to 2D imaging and is not easily adaptable to 3D imaging due to a larger outflow volume. MSDE provides several advantages, such as cancelling blood flow signals in any direction without impacting the scan time. This technique has been demonstrated to reduce plaque-mimicking flow artifacts in the carotid bifurcation, an area where the blood signal suppression is frequently imperfect [22]. However, the MSDE technique tends to introduce T2 decay and diffusion attenuation, leading to an overall SNR and contrast drop across the image. This signal attenuation can restrict the use of MSDE for high-resolution vascular imaging where SNR is already low, even at 3T.

An improved black-blood technique called Delay Alternating with Nutation for Tailored Excitation (DANTE)² has recently been proposed [23] as an alternative to MSDE, providing less SNR and T2 weighting loss without any impact on the acquisition time. This technique has the advantage of being independent of the 3D volume size, without being sensitive to inflow or outflow effects. It uses a train of low-flip-angle pulses interleaved with dephasing gradients to suppress flowing spins. The DANTE blood flow suppression efficiency has been demonstrated for several applications, such as carotid arteries and vessel wall imaging [24, 25] evaluations.

Removal of FID artifacts by simple averaging

The SPACE sequence uses variable-flip-angle refocusing RF pulses for extending the echo-train duration and reducing power deposition. However, like many things in MRI, the advantages of variable-flip-angle refocusing RF pulses also come with a potential problem – free-induction-decay (FID) artifacts [16]. An RF pulse with an intermediate flip-angle value plays three roles: excitation (to generate transverse magnetization), refocusing (to generate a spin-echo), and store/recall (to generate a stimulated echo). Therefore, if the flip angles of the refocusing RF pulses are not equal to 180°, longitudinal magnetization that regrows due to T1 relaxation during the time period between the excitation and first refocusing RF pulses, or between successive refocusing RF pulses, will be converted to transverse magnetization by the next refocusing RF pulse that is applied, and will thereby create an FID signal. While FID artifacts can be minimized by using fat saturation, or by increasing the readout crusher gradients at the expense of the echo-spacing, they can only be completely eliminated by simple signal averaging, alternating the phase of the refocusing RF pulses by 180° between averages. Scantime increase can be remedied by using higher acceleration factors, but at the expense of SNR due to the g -factor.

Iterative Denoising

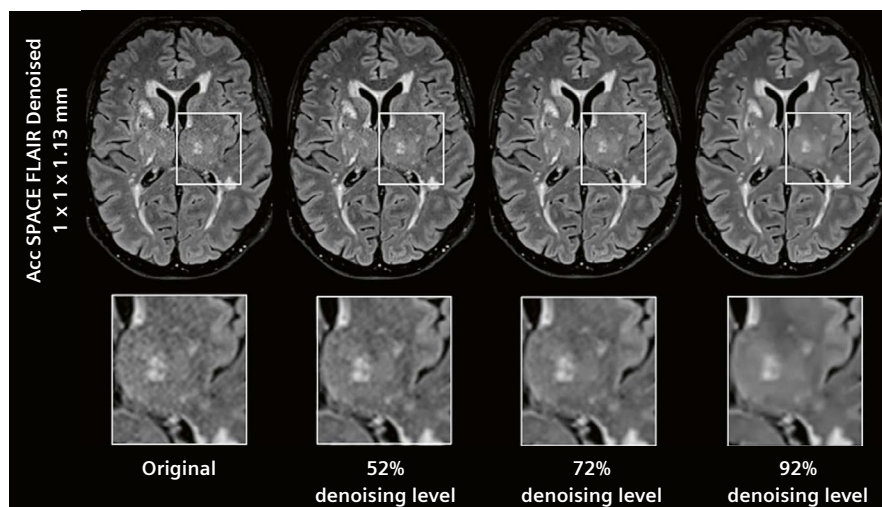
A prototype iterative denoising algorithm², which consists of an inner core of multiwavelet thresholding as a regularizer, was integrated into the scanner reconstruction pipeline [26]. During the iterations, the current regularized image was optimally combined with the original image and the previous image estimate, according to Stein's unbiased risk estimator [27]. The algorithm works on complex-valued 3D volumes after channel combination, considering the spatially varying noise level in the image, the g -factor from parallel imaging, and k -space filter functions. Patient-specific noise distribution was measured via a pre-scan by the system and was used as a quantitative input during reconstruction. Where appropriate, some edge enhancement was applied after the denoising stage to compensate for perceived loss in sharpness.

The denoising strength can be adapted by the user according to the physician's needs, as shown in Figure 2. It is important to mention, though, that the iterative denoising algorithm automatically adapts to changes in the acquisition and reconstruction settings, including RF coil properties, via the noise measurements. Therefore, the denoising strength should not require application-specific manual tuning.

To our knowledge, the ID algorithm has not been evaluated in combination with SPACE readout for neurological diseases. In this work we propose

- to optimize signal and contrast for different image weightings by means of the above mentioned preparation schemes (T2 preparation and DANTE) and
- to propose a well-designed use of moderate-to-high CAIPIRINHA acceleration factors in combination with the iterative denoising reconstruction algorithm.

²Work in progress: the application is currently under development and is not for sale in the U.S. and in other countries. Its future availability cannot be ensured.



2 Impact of the denoising strength effect on image quality and appearance. For clinical examination, a value of 72% has been chosen at Lariboisiere Hospital for the Accelerated SPACE FLAIR protocol.

Clinical experience with Iterative Denoising applied to the SPACE CAIPIRINHA sequence in Neurology

All patient images were obtained using a 3T MR scanner (MAGNETOM Skyra or Prisma, Siemens Healthcare, Erlangen, Germany) with a 64-channel Head&Neck coil. The prototype sequence consisted of a 3D SPACE CAIPIRINHA product implementation, combined with investigational magnetization preparation schemes and an inline iterative denoising reconstruction giving access to native image reconstruction and iteratively denoised image series.

As the presented results were obtained at different clinical sites, only spatial resolution and scan time are reported in Table 1 for the different applications and contrasts. For more information about the sequence parameters, please contact the corresponding authors. All FLAIR and DIR images were acquired using a short T2 preparation duration of 125 ms, followed by standard non-selective inversion pulses with specific inversion times to null the CSF, or two non-selective inversion pulses to suppress CSF and WM.

Accelerated SPACE FLAIR in brain tumor

FLAIR is considered the most important sequence in brain examinations as it provides an excellent lesion visualization. Blood flow artifacts and partial volume effects of 2D imaging can be addressed with a 3D volume dataset acquisition. The use of a non-selective inversion pulse in 3D imaging avoids flow related CSF artifacts (e.g., in the subarachnoid space and ventricles) that commonly occur in 2D-based methods. However, the use of 3D in clinical routine is limited by its longer acquisition time over 2D imaging.

Figure 3 shows an example of a 68-year-old woman who was referred for follow-up exam of a cavernoma. A standard transversal 3D SPACE FLAIR of about 5 minutes scan time was acquired for comparison. Here, the use of a

highly accelerated 3D SPACE FLAIR reconstructed with ID maintains a high image quality and a voxel size close to 1 mm³ with a scan time reduction of 37%. At Lariboisière neuroradiology department, approximately 110 patients undergo brain screening MRI sequences per week. This means that an additional scan time of 3 hours per week is provided only by integrating ID on 3D FLAIR sequences.

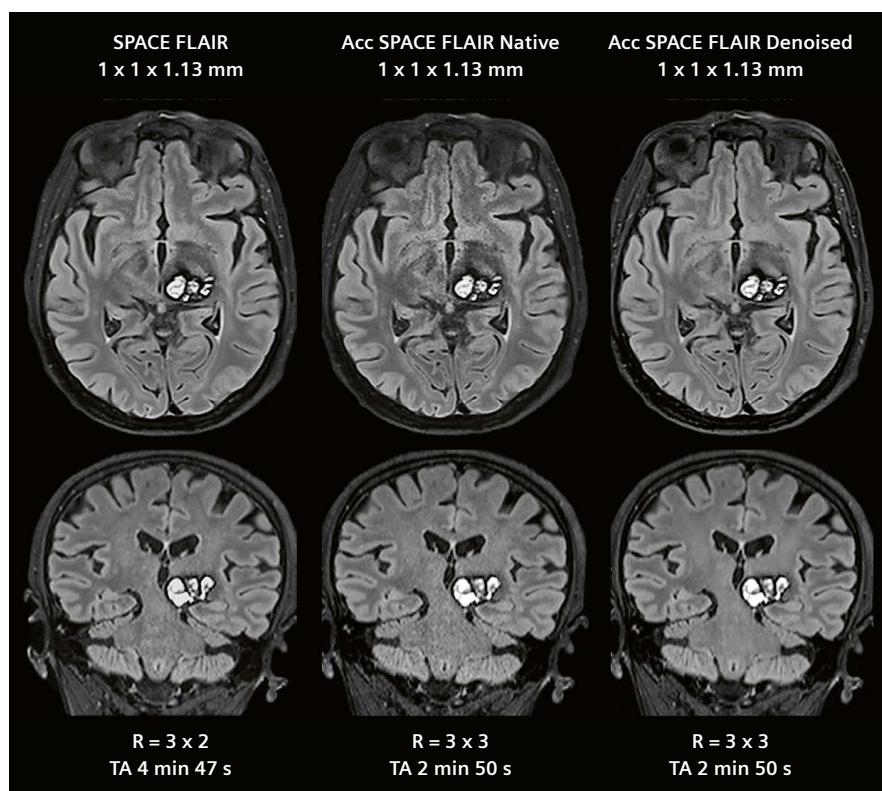
Improved spatial resolution and contrast in multiple sclerosis

In multiple sclerosis (MS) and other inflammatory neurological disorders, FLAIR is also considered the most important contrast for lesion assessment and follow-up. 3D imaging with isotropic voxel size is essential to limit partial volume effect, especially as there is an increasing interest in cortical and juxta-cortical abnormalities in MS. Detection of WM and GM lesions requires high spatial resolution and excellent contrast and SNR. By combining T2 magnetization preparation to improve the lesion's contrast with the ID reconstruction technique, it is possible to achieve a 0.8 mm isotropic 3D SPACE FLAIR in a clinically acceptable imaging time of about 5 minutes (Fig. 4). Until now, this spatial resolution for FLAIR imaging has only been reported at higher field strengths such as 7 Tesla.

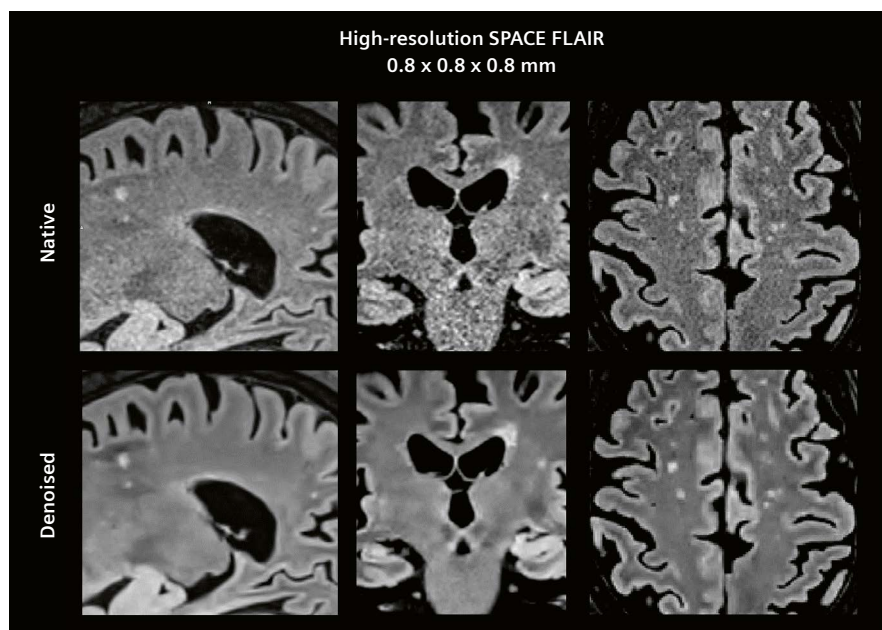
Double-Inversion Recovery sequences have been shown to be more sensitive for the assessment of MS lesion or optic neuritis. However, the DIR preparation strongly reduces the remaining MR signal for the readout module, which makes this technique highly challenging and unstable for use in clinical practice. Indeed, standard reported 3D SPACE DIR sequences usually necessitate a scan time of more than 6 minutes for decent image quality. A strongly accelerated high-resolution SPACE DIR acquired in 3 minutes and 40 seconds on an MS patient is presented in Figure 5. This figure also presents the high-resolution coronal and transversal FLAIR reformats, with a scan time reduction of around 40% for both sequences.

Sequence & Site	Spatial Resolution (mm)	CAIPIRINHA Acceleration Factor	Scan Time
Standard Space_FLAIR_Lariboisiere	1 x 1 x 1.13	3 x 2 (2 avg)	4 min 47 s
Accelerated Space_FLAIR_Lariboisiere	1 x 1 x 1.13	3 x 3 (2 avg)	2 min 50 s
High-resolution Space_FLAIR_Montpellier	0.8 x 0.8 x 0.8	4 x 3 (2 avg)	5 min 20 s
High-resolution Space_DIR_Montpellier	0.9 x 0.9 x 1.2	3 x 2	3 min 40 s
High-resolution_Space_T1/T1 DANTE_CHNO	0.8 x 0.8 x 0.8	3 x 2 (2 avg)	4 min 34 s

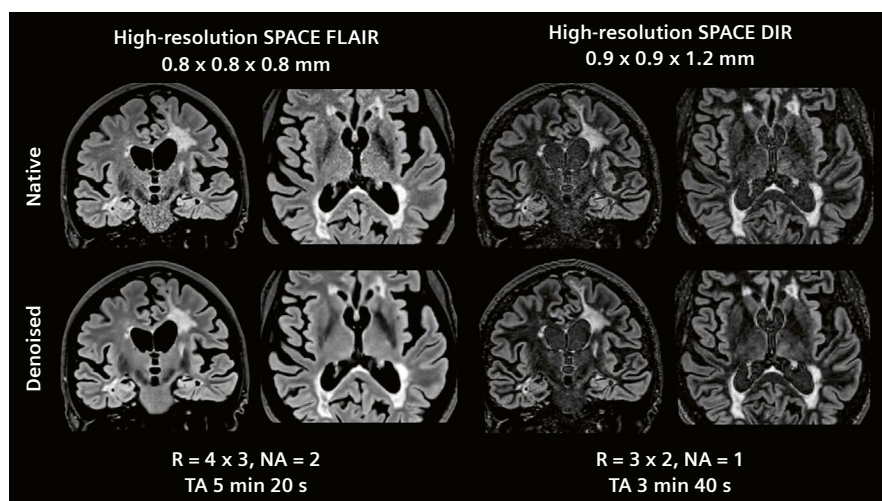
Table 1: Principal sequence parameters for the different sites and applications.



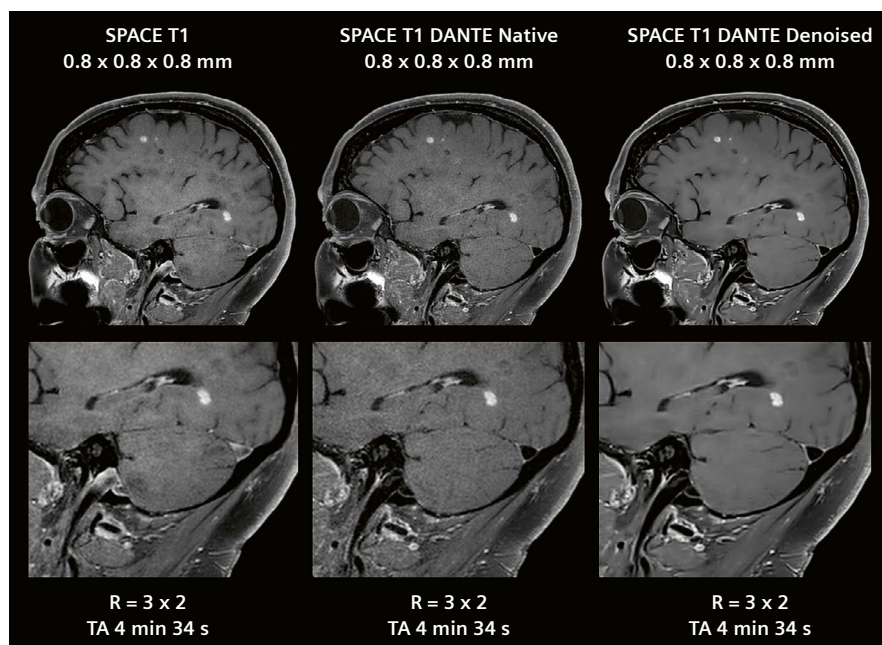
- 3** A 68-year-old woman was referred for follow-up of a cavernoma to Lariboisiere University Hospital Center (Paris, France). A standard Axial 3D SPACE FLAIR was acquired with an in-plane resolution of 1 mm in 4 min 47 s (left). The use of a higher acceleration factor dramatically decreases the SNR level especially in the image center (middle). After reconstruction with ID, the accelerated 3D SPACE FLAIR highlights a similar image quality as the conventional sequence with a decreased scan time of 37%.



- 4** A 68-year-old male with suspected autoimmune encephalitis was referred to Montpellier University Hospital. High resolution T2-prepared SPACE FLAIR images were acquired with an isotropic voxel of 0.8 mm. Conventional reconstructions are shown on the upper row with a SNR reduction that impedes clinical diagnosis. Iterative denoising (lower row) allows the same high spatial resolution with an enhanced SNR.



- 5** A 58-year-old female with multiple sclerosis was referred to Montpellier University Hospital. High resolution T2-prepared SPACE FLAIR and DIR images were acquired. Coronal and transversal reformat are shown with and without ID. Thanks to ID, FLAIR, and DIR are both acquired with a high spatial resolution, a high SNR and an acquisition time remaining compatible with clinical routine.



- 6** A 37-year-old woman was referred for follow-up of multiple brain metastases to the Centre Hospitalier National d'Ophthalmologie des Quinze-Vingts (Paris, France). A conventional post contrast SPACE T1 sequence acquired with a spatial resolution of 0.8 mm³ (left) exhibits flow related artifacts enhancement in the carotid aera and the right sinus as well as a high SNR drop. With DANTE preparation (middle), both flow related artifacts are corrected. The additional ID reconstruction (right) highlights a much sharper image quality and compensate the low SNR level of the native sequence.

Improved spatial resolution and contrast in brain metastasis

In vascular neuro MR, wall-thickening and mural-enhancement evaluations are challenging because of the tortuous course and small dimensions of the intracranial arterial vessels. The use of a high resolution and isotropic 3D SPACE T1 black-blood imaging is mandatory to reformat and analyze their whole courses; this therefore provides a larger and better imaging coverage than conventional

2D sequences. Moreover, the combination of an additional DANTE preparation can suppress residual blood flow and improves brain metastasis conspicuity [28]. The combination of a DANTE preparation with an ID reconstruction is proposed as an efficient method to provide a 0.8 mm isotropic sequence while maintaining scan time below 5 minutes, as shown in Figure 6.



Acquisition speed ... what for?

Despite the development of new acceleration techniques over the past decades, fast brain MR examinations remain an ongoing topic to improve patient comfort, exam reproducibility, and the cost effectiveness of the MRI unit. Indeed, motion-related artifacts and image blurring hamper diagnostic quality, especially with uncooperative patients or in pediatric³ populations. Several developments have already been proposed, such as the GOBrain protocol [29] that include fast and individual 2D sequence optimizations to provide an accurate diagnosis in less than 5 minutes. However, the advantage of 3D over 2D imaging has already been largely described for neurological diseases: providing thinner and contiguous slices, overcoming partial volume effect, and allowing for multiplanar image reconstruction with a high sensitivity in lesion detection. The longer acquisition time of 3D compared to 2D remains the major drawback that limits its general usage.

The use of CS to address this issue remains limited by the relatively low acceleration rates achievable, which does not exceed 3 to 4-fold for 3D static neuro imaging. CS is also limited by its extended reconstruction time, which increases with the number of coil elements, especially during whole-brain acquisition with a 64-channel head coil. The reconstruction time can be reduced with the use of Graphic Process Unit but not all clinical MR scanners are currently equipped with one, and the widespread use of CS sequences remains limited. While CS iterates on multi-channel under-sampled *k*-space data, the ID algorithm iterates on images after coil combination, i.e., a reduced amount of data. For that reason, it can be performed on conventional computers without noticeable reconstruction time increase. Finally, the use of a quantitative noise map acquired during the framework adjustment is particularly suited to limit the *g*-factor penalty associated with high acceleration rates. As a result, the final images after ID do not suffer from central SNR drop and ensure a near perfect receive-B₁ image homogeneity.

In this work, a novel iterative denoising technique was successfully evaluated for 3D brain imaging in different clinical questions. Combined with the SPACE sequence, the ID algorithm ensures excellent image quality regardless of the image contrast. Furthermore, its application on conventional Cartesian datasets allows the use of 6- to 12-fold acceleration rates without compromising image quality. Several optimizations were proposed for different pathologies and clinical needs. For instance, tumor follow-up exams can be performed with a fast millimetric 3D scan, improving the overall patient throughput. On the other hand, small MS lesions can only be depicted with

sub-millimetric 3D scans, that are usually not possible on 3T systems. Similarly, as intra-cranial blood vessels range from a few millimeters to capillaries, the higher the spatial resolution is, the more sensitive the scan will be. Improving spatial resolution while keeping the scan time under 5 minutes will not only maintain a constant total exam time, but will also help to move toward precision medicine and dedicated high-resolution scans when needed for the patient. The gain in acquisition speed can also be invested in acquiring additional scans that are beneficial for the patient, such as an additional DIR contrast as presented here, or quantitative T1 and T2 maps that can then be compared to a normative database.

In order to validate the use of ID in clinical routine, future work will focus on the quantitative evaluation of these contrast-optimized and highly accelerated sequences in patient cohorts. The acceleration capabilities could be further expanded by combining the iterative denoising reconstruction algorithm with more advanced Cartesian 3D acceleration such as the recently proposed Wave-CAIPI [30, 31]. The combination of both techniques would push the acceleration capabilities of the SPACE sequence even further, without SNR penalty.

Acknowledgments

The authors would like to thank their colleagues at Siemens Healthineers who participated in the project: Michael Hamm and Andreas Schaeffer for project initialization and artifact analysis in the SPACE FLAIR sequence, and Xiaoming Bi for the DANTE preparation scheme implementation. The iterative denoising framework was developed by Stephan Kannengiesser and Boris Mailhe. We also thank Tobias Kober and Aurélien Monnet for the fruitful discussions on 3D anatomical brain imaging and FLAIR optimization.

References

- 1 Pruessmann KP, Weiger M, Scheidegger MB, Boesiger P. SENSE: sensitivity encoding for fast MRI. *Magn Reson Med.* nov 1999;42(5):952-62.
- 2 Griswold MA, Jakob PM, Heidemann RM, Nittka M, Jellus V, Wang J, et al. Generalized autocalibrating partially parallel acquisitions (GRAPPA). *Magn Reson Med.* juin 2002;47(6):1202-10.
- 3 Robson PM, Grant AK, Madhuranthakam AJ, Lattanzi R, Sodickson DK, McKenzie CA. Comprehensive quantification of signal-to-noise ratio and *g*-factor for image-based and *k*-space-based parallel imaging reconstructions. *Magn Reson Med.* oct 2008;60(4):895-907.
- 4 Breuer FA, Blaimer M, Heidemann RM, Mueller MF, Griswold MA, Jakob PM. Controlled aliasing in parallel imaging results in higher acceleration (CAIPIRINHA) for multi-slice imaging. *Magn Reson Med.* mars 2005;53(3):684-91.
- 5 Breuer FA, Blaimer M, Mueller MF, Seiberlich N, Heidemann RM, Griswold MA, et al. Controlled aliasing in volumetric parallel imaging (2D CAIPIRINHA). *Magn Reson Med.* mars 2006;55(3):549-56.

³MR scanning has not been established as safe for imaging fetuses and infants less than two years of age. The responsible physician must evaluate the benefits of the MR examination compared to those of other imaging procedures.

- 6 Breuer F, Blaimer M, Griswold M, Jakob P. Controlled Aliasing in Parallel Imaging Results in Higher Acceleration (CAIPIRINHA). MAGNETOM Flash · 1/2012.
- 7 Donoho DL. Compressed sensing. IEEE Trans Inform Theory. avr 2006;52(4):1289-306.
- 8 Lustig M, Donoho D, Pauly JM. Sparse MRI: The application of compressed sensing for rapid MR imaging. Magn Reson Med. déc 2007;58(6):1182-95.
- 9 MAGNETOM Flash Magazine – Compressed Sensing Supplement (66) 3/2016.
- 10 Yang AC, Kretzler M, Sudarski S, Gulani V, Seiberlich N. Sparse Reconstruction Techniques in Magnetic Resonance Imaging: Methods, Applications, and Challenges to Clinical Adoption. Investigative Radiology. juin 2016;51(6):349-64.
- 11 Setsompop K, Cohen-Adad J, Gagoski BA, Raij T, Yendiki A, Keil B, et al. Improving diffusion MRI using simultaneous multi-slice echo planar imaging. NeuroImage. oct 2012;63(1):569-80.
- 12 Sharma SD, Fong CL, Tzung BS, Law M, Nayak KS. Clinical Image Quality Assessment of Accelerated Magnetic Resonance Neuroimaging Using Compressed Sensing: Investigative Radiology. sept 2013;48(9):638-45.
- 13 Sartoretti T, Reischauer C, Sartoretti E, Binkert C, Najafi A, Sartoretti-Schefer S. Common artifacts encountered on images acquired with combined compressed sensing and SENSE. Insights Imaging. déc 2018;9(6):1107-15.
- 14 Toledano-Massiah S, Sayadi A, de Boer R, Gelderblom J, Mahdjoub R, Gerber S, et al. Accuracy of the Compressed Sensing Accelerated 3D-FLAIR Sequence for the Detection of MS Plaques at 3T. AJNR Am J Neuroradiol. mars 2018;39(3):454-8.
- 15 Vranic JE, Cross NM, Wang Y, Hippe DS, de Weerd E, Mossa-Basha M. Compressed Sensing – Sensitivity Encoding (CS-SENSE) Accelerated Brain Imaging: Reduced Scan Time without Reduced Image Quality. AJNR Am J Neuroradiol. janv 2019;40(1):92-8.
- 16 Mugler JP. Optimized three-dimensional fast-spin-echo MRI: Optimized 3D Fast-Spin-Echo MRI. J Magn Reson Imaging. avr 2014;39(4):745-67.
- 17 Visser F, Zwanenburg JJM, Hoogduin JM, Luijten PR. High-resolution magnetization-prepared 3D-FLAIR imaging at 7.0 Tesla: Magnetization-Prepared 3D-FLAIR Imaging at 7T. Magn Reson Med. juill 2010;64(1):194-202.
- 18 Saranathan M, Worters PW, Rettmann DW, Winegar B, Becker J. Physics for clinicians: Fluid-attenuated inversion recovery (FLAIR) and double inversion recovery (DIR) Imaging: FLAIR and DIR Imaging. J Magn Reson Imaging. déc 2017;46(6):1590-600.
- 19 Park J, Mugler JP, Horger W, Kiefer B. Optimized T1-weighted contrast for single-slab 3D turbo spin-echo imaging with long echo trains: Application to whole-brain imaging. Magn Reson Med. nov 2007;58(5):982-92.
- 20 Reichert M, Morelli JN, Runge VM, Tao A, von Ritschl R, von Ritschl A, et al. Contrast-Enhanced 3-Dimensional SPACE Versus MP-RAGE for the Detection of Brain Metastases: Considerations With a 32-Channel Head Coil. Investigative Radiology. janv 2013;48(1):55-60.
- 21 Thaler C, Schneider T, Sedlacik J, Kutzner D, Stellmann J-P, Heesen C, et al. T1w dark blood imaging improves detection of contrast enhancing lesions in multiple sclerosis. Meckel S, éditeur. PLoS ONE. 10 août 2017;12(8):e0183099.
- 22 Wang J, Yarnykh VL, Hatsukami T, Chu B, Balu N, Yuan C. Improved suppression of plaque-mimicking artifacts in black-blood carotid atherosclerosis imaging using a multislice motion-sensitized driven-equilibrium (MSDE) turbo spin-echo (TSE) sequence. Magn Reson Med. nov 2007;58(5):973-81.
- 23 Li L, Miller KL, Jezard P. DANTE-prepared pulse trains: A novel approach to motion-sensitized and motion-suppressed quantitative magnetic resonance imaging: DANTE-Prepared Pulse Trains. Magn Reson Med. nov 2012;68(5):1423-38.
- 24 Li L, Chai JT, Biasioli L, Robson MD, Choudhury RP, Handa AI, et al. Black-Blood Multicontrast Imaging of Carotid Arteries with DANTE-prepared 2D and 3D MR Imaging. Radiology. nov 2014;273(2):560-9.
- 25 Xie Y, Yang Q, Xie G, Pang J, Fan Z, Li D. Improved black-blood imaging using DANTE-SPACE for simultaneous carotid and intracranial vessel wall evaluation: DANTE-SPACE for Simultaneous Carotid and Intracranial Vessel Wall Imaging. Magn Reson Med. juin 2016;75(6):2286-94.
- 26 Kannengiesser SA, Mailhe B, Nadar M, et al. Universal iterative denoising of complex-valued volumetric MR image data using supplementary information. ISMRM. 2016.
- 27 Luisier F, Blu T, Unser M. SURE-LET for Orthonormal Wavelet-Domain Video Denoising. IEEE Trans Circuits Syst Video Technol. juin 2010;20(6):913-9.
- 28 Suh CH, Jung SC, Kim KW, Pyo J. The detectability of brain metastases using contrast-enhanced spin-echo or gradient-echo images: a systematic review and meta-analysis. J Neurooncol. sept 2016;129(2):363-71.
- 29 Rapalino O, Heberlein K. New Strategies for Protocol Optimization for Clinical MRI: Rapid Examinations and Improved Patient Care. MAGNETOM Flash – 2/2016.
- 30 Bilgic B, Gagoski BA, Cauley SF, Fan AP, Polimeni JR, Grant PE, et al. Wave-CAIPI for highly accelerated 3D imaging: Wave-CAIPI for Highly Accelerated 3D Imaging. Magn Reson Med. juin 2015;73(6):2152-62.
- 31 Filho A, Conklin J, Rapalino O, Schaefer P, Huang S. Ultrafast Multi-contrast High-resolution 3D Brain MRI: a Technical Description of Wave-CAIPI. MAGNETOM Flash 1/2020.

Contact

Alexis Vaussy
Siemens Healthcare SAS
40 Avenue des Fritiers
93210, Saint Denis
France
alexis.vaussy@siemens-healthineers.com



Thomas Troalen
Siemens Healthcare SAS
40 Avenue des Fritiers
93210, Saint Denis
France
thomas.troalen@siemens-healthineers.com



Experience of Using a New Autopilot Assistance System for Easy Scanning in Brain and Knee MRI Examinations

Tanja Dütting, M.D.; Stephan Clasen, M.D.

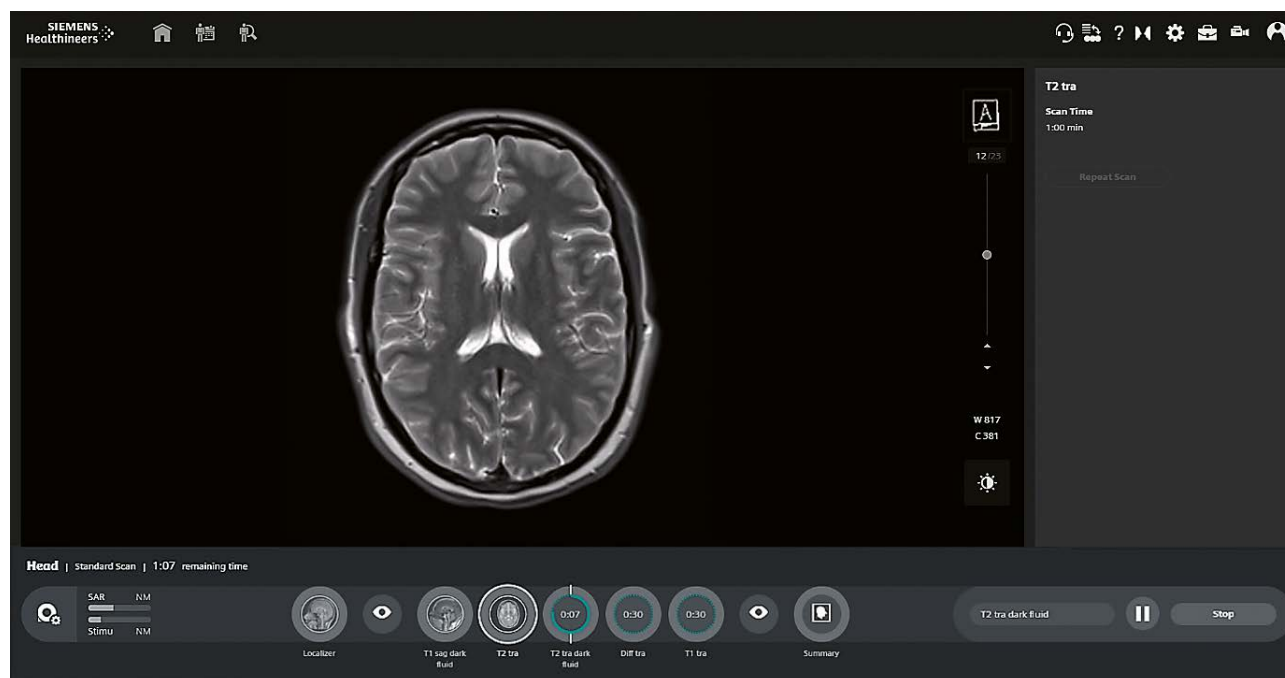
Institute for Diagnostic and Interventional Radiology, Kreiskliniken Reutlingen, Germany

Context

The number of diagnostic MRI examinations is rising at a time when cost pressure is high in radiology. As a result, workloads are increasing. Imaging providers are therefore looking for new solutions that will deliver high quality care at optimized, low costs (= productivity) and enable more employees to carry out the examinations. Since qualified staff is expensive and, in some places, hard to find, technological advancements could become the key to success for reproducible magnetic resonance imaging.

New scanning assistance systems are needed if radiologists and imaging providers are to cope with the increasing demand and the high expectations of quality while only having a limited workforce.

We report on our initial experiences with a new technology, myExam Autopilot, to describe the possibilities offered by the novel solution. The focus was on standard brain and knee MRI examinations, which account for a large share of routine examinations.



1 Screenshot of the myExam Autopilot prototype showing the simplified and more intuitive user interface for a brain scan.



Aims

- To evaluate the scope for enabling low-skilled and inexperienced radiology technologists to perform reproducible, standardized MRI examinations of the brain and knee with no specific training and no individual support
- To evaluate whether the automation gives experienced users more time for other tasks

myExam Autopilot: Background

New automated scanner software has recently been developed and will be tested for brain and knee MRI examinations: myExam Autopilot for the brain and knee offers fast, reproducible, and standardized MRI examinations. It supports multiple exam strategies (e.g., standard, fast, standard with contrast agent) so that the strategy can be adapted to the local situation. The aim is to use the advanced workflow automation for standardized scan volume positioning, tilting, and coverage in order to achieve a high degree of consistency between examinations and to provide better support for inexperienced users.

Consequently, myExam Autopilot completely removes the need for individual users to manually adjust

the protocols. It also features a greatly simplified and therefore more intuitive user interface. The system guides users through an automated workflow that allows them to scan intuitively, while artificial intelligence helps set the slice position, tilt, number of slices, and the individual examination steps: After entering the patient data, the preselected exam card opens automatically. The AutoAlign Localizer starts at the touch of a button. It provides landmarks and orientation for automatic positioning of the slices in a standardized way independent of the operator. AutoCoverage ensures the anatomy under examination is covered consistently throughout the entire examination. The myExam Autopilot program uses this information to automatically plan the preprogrammed sequences and then allows them to run. Overall, the user has to do very little.

Method

We evaluated myExam Autopilot in a test phase from June to August 2020. We investigated 24 routine examinations of the brain and eight examinations of the knee joint using standard MRI that was pre-configured with fixed sequences. The examinations were performed by six different users, three of whom were inexperienced.

Dot Engine vs. myExam Autopilot

myExam Autopilot provides user assistance and automation beyond the current Dot technology.

Dot Engine:

- Automatic planning powered by AI
- Standardized examination protocols, adaptable to institutional needs
- Possibility to set-up scan strategies and decisions

myExam Autopilot adds further functionalities:

- MRI at the click of a button
- Automated protocol without the need for manual adjustment
- Drastically simplified user interface (touch screen supported)
- Visual user guidance text, e.g., for image QA

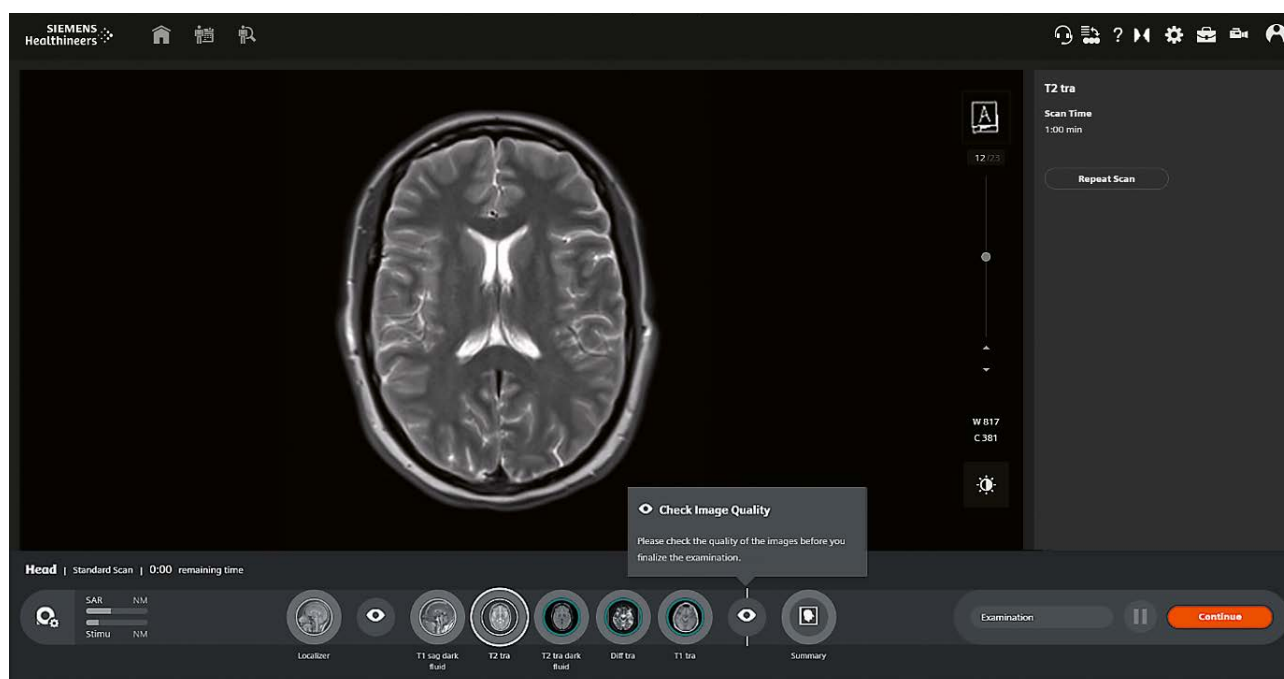
The inexperienced group included users of different modalities, e.g., CT, who are rarely involved in performing MRI examinations.

The standard sequences were as follows:

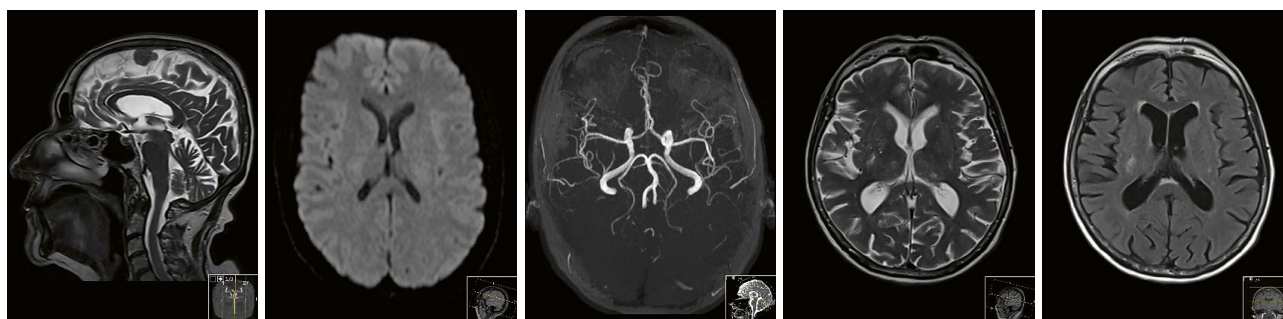
- Brain: transverse Dark Fluid, transverse T2-TSE, transverse DWI, transverse T1-SE, transverse T2-GRE, sagittal T2-TSE, sagittal DWI, TOF angiography of the circle of Willis.
- Knee: sagittal PD FS-TSE, sagittal PD-TSE, coronal and transverse PD FS-TSE, coronal T1-TSE.

Results

All users had a positive initial impression of myExam Autopilot and were confident using it. They needed just a brief introduction to be able to use the software, and were familiar with its operation after using it just once or twice. The three inexperienced users liked the user-friendliness and felt that the workflow was easier and required less effort. They were able to use the program after a brief introduction and no extra training. As their uncertainty regarding the complexity of conventional scan protocols was no longer an issue, they also saved time during the examination.



2 Screenshot of the prototype showing integrated guidance text in the workflow. Further support is provided by automatic planning from AutoAlign and AutoCoverage for consistent slice or volume coverage and orientation.



3 A brain MRI examination with myExam Autopilot performed by an inexperienced user.

For the three experienced users, the new workflow was unfamiliar and offered less scope for making manual adjustments. For them, it was helpful and important to be able to switch to the conventional user interface (myExam Assist) so that they could change or supplement sequences, if required for the individual case. As a result, the experienced users spent similar time on scanning and system operations as the unexperienced group. Additional myExam Autopilot exam strategies could reduce individual adjustments so that experienced users could also benefit from time savings. This remains to be evaluated further.

Both user groups were able to achieve high quality diagnostic results which were evaluated by the radiologists involved in this study. The diagnostic results of the new program provided the same quality as the original Dot Engine software.

The automation of the myExam Autopilot software worked reliably and delivered consistent results in both groups. The slice groups were correctly positioned in all examinations. The sequences ran without error and image reconstruction occurred promptly.

One issue that the experienced users felt should be addressed was that inexperienced users were less critical of the automated exam and accepted it without checking it or, if necessary, supplementing it or repeating blurred sequences. This issue could be resolved by raising awareness through training.

Discussion

Given the aims of the evaluation, the following conclusions can be drawn:

- myExam Autopilot helps less experienced users to carry out MRI scans with consistently high image quality.
- myExam Autopilot is an intelligent solution that addresses the increasing global demand for MRI examinations.

It is a very stable, reliable method for performing routine exams of the brain or the knee. The automatic positioning is very robust and almost entirely unsusceptible to errors. Performing a standard exam is easy to learn and requires just a few steps and minimal interaction. myExam Autopilot makes particular sense in scenarios such as occupational medical examinations performed by technologists who do not normally use MRI workstations, and standard MRI examinations that are carried out in regions with limited access to MRI and no access to staff with specific MRI training. myExam Autopilot is currently being expanded to include spine MRI exams, which are also increasingly in demand. This will be a welcome addition to the technology.



Professor Dr. Stephan Clasen



Dr. Tanja Dütting

Contact

Dr. Tanja Dütting, M.D.
Senior Physician
Institute for Diagnostic and Interventional Radiology
Kreiskliniken Reutlingen
Steinenbergstraße 31
72764 Reutlingen
Germany
Duetting_t@klin-rt.de

MAGNETOM Free.Max: from Concept to Product, a Brief History of the DryCool Magnet Development

Simon Calvert, CEng FIMechE

Head of Product Innovation & Chief Technology Officer, Siemens Healthineers, Oxford, UK

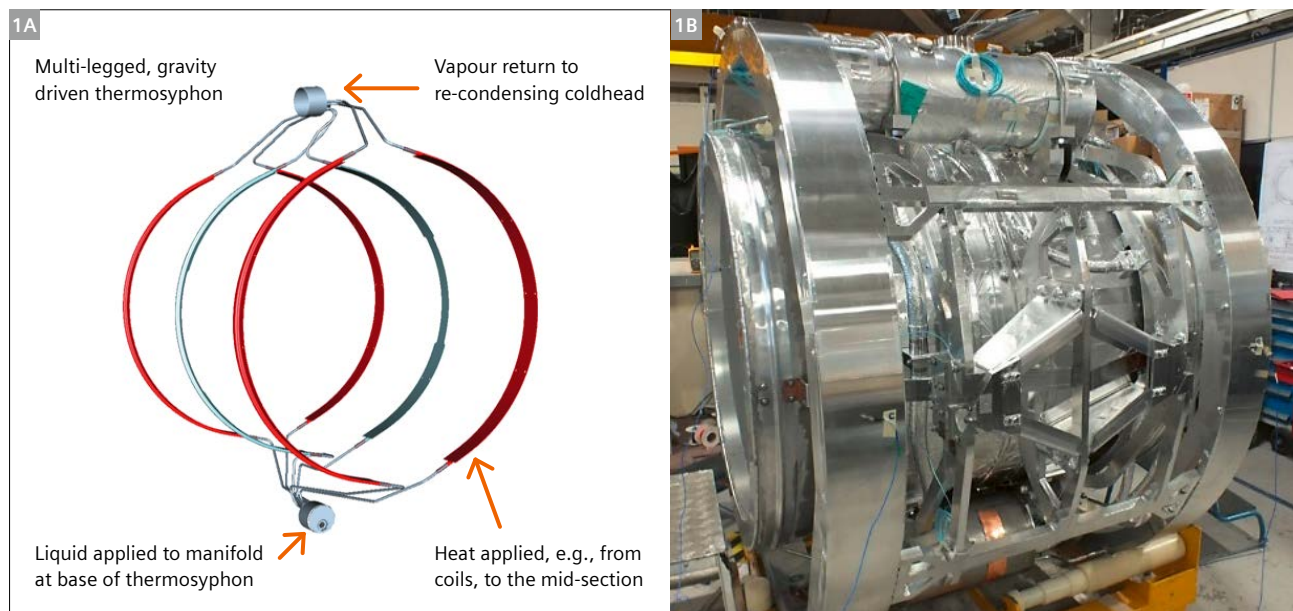
Introduction

Our new DryCool magnet is a key enabling element of our ground-breaking MAGNETOM Free.Max MRI system. The development and production program for the new generation magnet has lasted four years but was preceded by a research program lasting seven years, focussed on completely transforming and deploying new superconducting MRI magnet technologies. The program included developing new magnet coil technology and structural concepts as well as realising a dramatic reduction in our dependency on increasingly expensive, and sometimes scarce, liquid helium coolant. The highly innovative

technologies used in the DryCool magnet are complimentary, and deliver a robust, reliable, and lightweight “plug and play” magnet solution to you.

1.5T Minimum Helium Inventory (MHI) research program (2008–2015)

In 2008 we started a program to transform our magnet technology and to reduce our dependency on helium. A key requirement for conduction-cooled superconducting magnets is to minimize the mass of the cold parts of



1 1.5 Tesla demonstrator showing the cryogenic concept and the superconducting magnet structure. **(1B)** 4K mass during build.

MAGNETOM Free.Max is currently under development and is not for sale in the U.S. and in other countries. Its future availability cannot be ensured.

the structure. Our focus was to use only the magnet's own refrigerator to cool down to operating temperature, thus avoiding the requirement for complex installation procedures.

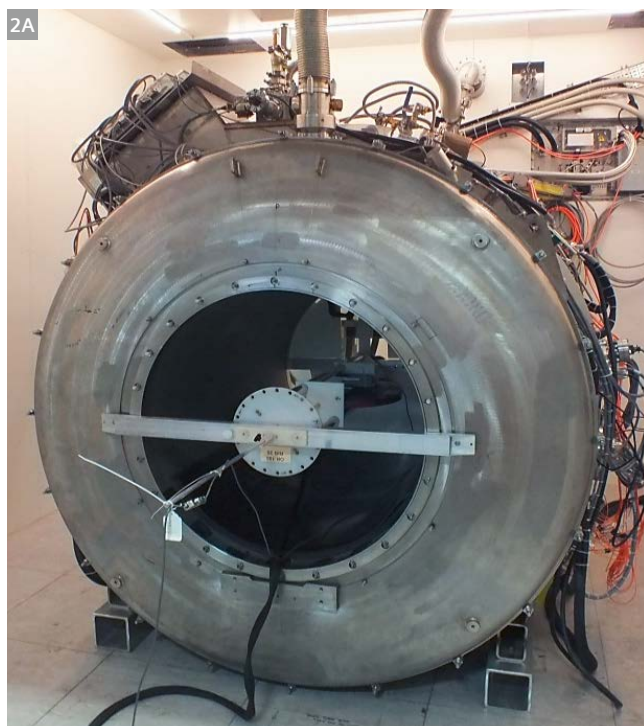
The focus of the research program was to realize a 1.5T "Minimum Helium Inventory" magnet, which could later be integrated into an MRI system for imaging trials. Half scale, pipe-cooled magnets were developed and tested to prove the various technical concepts which were to be used in the 1.5T demonstrator. All tests were successful, and these technologies were then incorporated into the full-size magnet. The demonstrator was not intended to lead directly to a product but was a testbed to evaluate our new ground-breaking technologies. The magnet worked reliably and was also extensively tested in a MAGNETOM Aera MRI system in 2014 where it performed as well as the conventional "wet" magnet. New magnet electronics and software concepts were also developed and evaluated as part of the 1.5T MHI demonstrator program.

Simplification and focus on manufacturability

A great deal was learnt from the 1.5T research program, including how to develop a "dry" magnet which was optimized for cost and manufacturability. Much was also learnt about how conduction-cooled magnets interact with the MRI system and, in particular, the gradient system.

DryCool magnet development program (2016–2020)

The DryCool magnet development program was kicked off using the learnings from the 1.5T research program. Here, numerous aspects were considered for a design in order to maximize clinical utility while at the same time minimize the requirements on site infrastructure. The result of this development is a newly designed magnet unlike any Siemens Healthineers has built before. The new DryCool design enabled us to keep the mass low, allowing not only for shorter cool-down times, but also reduce installation costs. This will clearly make it easier to site this magnet at non-traditional sites. Additionally, a new field strength was considered in the DryCool design to allow for greater clinical flexibility. The chosen field strength of 0.55T allows just that. Lower fields show better compatibility when it comes to implants or interventional devices such as catheters. Anatomical regions such as the lung, have been traditionally off-limits for MRI at conventional field strengths. Lower field strengths can make MRI more versatile in this respect as well. Finally – patients benefit from the DryCool design: with an 80 cm bore, patients will experience an openness in MRI that no other whole body superconducting magnet can offer. All of these elements come into play with the DryCool Magnet design.



2 1.5 Tesla demonstrator during magnet testing and MRI system testing in 2014. (2A) Magnet tests in Oxford. (2B) System tests in Erlangen.



3 Prototype
DryCool 0.55
Tesla magnet

DryCool magnet specification

• Field strength:	0.55 Tesla
• Field temporal stability:	< 0.1 ppm/hour
• 5 gauss contours (from isocentre):	Axial 4.0 m, Radial 2.5 m
• Homogeneity:	See table 1
• Magnet length:	1.48 m
• Magnet warm bore:	1.060 m
• Magnet mass (installed):	1635 kg
• Liquid helium inventory:	0.7 litres (under normal operation)
• Helium boil-off rate:	Zero (under all imaging conditions)
• Cryogenic system:	Sealed helium system, no quench line
• Cooldown time from warm:	< 14 days (using the magnet's refrigerator)
• Designed acceleration limits:	5g vertical, 2g lateral
• Magnet current leads:	Fixed leads with HTS elements
• Automatic ramp-down:	Yes, if refrigeration is off for a period.
• Auto ramp-up:	Yes. Controlled by the magnet supervisory.
• Remote monitoring of the magnet:	Yes. Diagnostics on magnet and refrigerator.



DryCool magnet features

Advanced superconducting magnet structure with very low mass

The new superconducting magnet structure has a mass of approximately 300 kg. To achieve this exceptionally low mass in a large bore, the actively shielded magnet required the use of several new and innovative technologies. A completely new structural concept was used for the coils and supporting structure which, while very robust, allowed the use of very thin, yet stiff, structures. Since the volume of superconductor in the coil is low, a new ultra-fast quench propagation system was also developed to ensure that the magnet was not damaged if the Emergency Run Down Unit (ERDU) button was pressed. New superconducting joints, superconducting switches and other components were also developed. These components are no longer immersed in liquid helium and so need to be cooled by conduction only. Another key aspect of the magnet structure was to ensure that the coils had very low heating due to interaction with the gradient coil. New and innovative technologies were adopted to ensure that gradient coil-induced heating of the coils was minimized, and subsequent testing showed that the approach adopted was highly effective.

Simplified, manufacturable, and robust DryCool cryogenic system

The 1.5 Tesla demonstrator magnet had a cryogenic system which used pipes encircling the superconducting structure. While quite effective, such a system is complex to manufacture with many joints in the helium system. For the DryCool magnet, we adopted a simpler and more robust approach which was suitable for manufacture in high volumes. The cryogenic package is a separate sub-system which is integrated into the superconducting magnet structure by use of an innovative and highly optimized thermal connection system. This system efficiently removes heat from the coils and supporting structure giving a fast cool-down time, a low base temperature, and excellent tolerance of gradient coil interaction. Even with the most challenging imaging sequences, there is minimal heating of the magnet coils. The cryogenic package contains 0.7 litres liquid helium and is sealed, and so requires no quench pipe. Charging of the helium system is by high pressure gas only and no liquid helium is required. Once charged, and provided with power, the magnet will automatically cool down to operating temperature in less than 14 days. If the magnet arrives at the installation site partially cold, as will often be the case, the cool down time will be shortened.

DryCool magnet cryostat

The magnet cryostat is the sub-system that keeps the magnet coils cold and well protected. It has been highly

optimized to minimize weight, minimize heat input to the superconducting magnet, and to ensure a high level of robustness during shipment, installation, or in seismic events when on site. Since we intend the DryCool magnet to be shipped to a wide range of locations across the globe, we have designed the cryostat to meet the same specifications as our wet magnets. The magnet can withstand sustained loads of 5g in the vertical direction and 2g in both lateral directions. This very robust specification ensures that the magnet is well protected during shipment to site.

Magnet electronics package and software

Since the DryCool magnet has a small inventory of helium and the heat capacity of most materials at 4 Kelvin is negligible, the tolerance of loss of refrigeration is less than a conventional "wet" magnet. Conventional superconducting magnets typically contain hundreds of litres of liquid helium and this gives a tolerance of refrigeration failure measured in days before magnet ramp-down is required. For the DryCool magnet, we have developed a sophisticated electronics and software system which monitors the magnet and refrigeration system and makes decisions about when to ramp the magnet down to avoid a quench. If the refrigeration system is off for a significant time period, the Magnet Supervisory and Control Unit (MSCU) will execute a magnet ramp down to avoid dissipating the magnet stored energy in the cold mass. The magnet energy is instead dissipated in a passive Run Down Load (RDL). Once the magnet has been run down, and the power and cooling water is available again, the RDL is actively cooled to reduce the temperature so that the magnet can be ramped back to field. The MSCU also monitors many other magnet parameters to determine when the magnet can be automatically ramped back to field. The magnet has an integrated Magnet Power Supply (MPS) which is used to automatically ramp the magnet to its precise current for field, before putting the magnet into persistent mode. The MSCU also monitors many magnet and refrigeration parameters which can be monitored remotely by our service organisation. This allows preventative maintenance to be planned to ensure maximum "uptime" for the magnet and MRI system.

Product Life Cycle (PLC) and

Total Cost of Ownership (TCO) savings

One key focus of the development of the DryCool magnet was to minimize Product Lifecycle Cost and Total Cost of Ownership for the customer. The very low magnet mass reduces the shipping costs, and reduces the logistics carbon footprint as, in many cases, sea or road shipments can be used rather than air freight. The low mass also reduces installation costs and allows the magnet to be

sited on upper floors. The low mass and small size of the magnet also allows the MAGNETOM Free.Max MRI system to be sited in non-traditional locations such as ER departments and clinics. The lack of a quench pipe further reduces the installation costs and enables the magnet to be sited in locations where quench pipe runs would be too long, or very difficult and expensive to install. The lack of a large helium inventory reduces the magnet purchase price and reduces the servicing costs for the customer. Since the magnet has its own magnet power supply, the customer can, in most cases, ramp the magnet up and down when required without a service visit being required.

Conclusions

The DryCool magnet is a highly innovative development which incorporates many new technologies and concepts. The magnet delivers the first 80 cm patient bore in the industry and is a key enabler for the ground-breaking MAGNETOM Free.Max MRI scanner. The magnet minimizes product life-cycle costs and total cost of ownership and virtually eliminates the complex superconducting magnet servicing procedures. The magnet is enabled for siting outside of traditional imaging suites and will undoubtedly help to extend the reach of MR not only into new locations, but also new clinical fields.

Contact

Simon Calvert
Siemens HC Ltd. MR Magnet Technology
SHS DI MR R&D MD
Wharf Road
OX29 4BP Oxford
United Kingdom
simon.calvert@siemens-healthineers.com



About Siemens Healthineers



At Siemens Healthineers, our purpose is to enable healthcare providers to increase value by empowering them on their journey toward expanding precision medicine, transforming care delivery, and improving patient experience, all enabled by digitalizing healthcare.

An estimated 5 million patients globally benefit every day from our innovative technologies and services in the areas of diagnostic and therapeutic imaging, laboratory diagnostics, and molecular medicine, as well as digital health and enterprise services.

We're a leading medical technology company with over 120 years of experience and 18,500 patents globally. With about 50,000 dedicated colleagues in over 70 countries, we'll continue to innovate and shape the future of healthcare.

The entire editorial staff at University Hospital Erlangen and at Siemens Healthineers extends their appreciation to all the radiologists, technologists, physicists, experts, and scholars who donate their time and energy – without payment – in order to share their expertise with the readers of MAGNETOM Flash.

MAGNETOM Flash – Imprint

© 2021 by Siemens Healthcare GmbH,
All Rights Reserved

Publisher:

Siemens Healthcare GmbH
Magnetic Resonance,
Karl-Schall-Str. 6, D-91052 Erlangen, Germany

Editor-in-chief:

Antje Hellwich
(antje.hellwich@siemens-healthineers.com)

Guest editors:

Professor Michael Uder, M.D.
Head of Department of Diagnostic and Interventional
Radiology, University Hospital Erlangen, Germany;
Professor Frederik B. Laun, Ph.D.,
Professor Armin M. Nagel, Ph.D.
MR Physics, University Hospital Erlangen, Germany

Editorial Board:

Rebecca Ramb, Ph.D.; Sunil Kumar S. L., M.D.;
Wellesley Were; Jane Kilkenny; Nadine Leclair, M.D.

Review Board:

André Fischer, Ph.D.; Daniel Fischer;
Giulia Ginami, Ph.D.; Heiko Meyer, Ph.D.;
Gregor Thörmer, Ph.D.

Copy Editing:

Sheila Regan, Jen Metcalf, UNIWORKS,
www.uni-works.org
(with special thanks to Kylie Martin)

Layout:

Agentur Baumgärtner,
Friedrichstr. 4, D-90762 Fürth, Germany

Production:

Norbert Moser,
Siemens Healthcare GmbH

Printer:

G. Peschke Druckerei GmbH,
Taxenstr. 4, D-85599 Parsdorf b. Munich, Germany

Note in accordance with § 33 Para.1 of the German Federal Data Protection Law: Despatch is made using an address file which is maintained with the aid of an automated data processing system.

MAGNETOM Flash is sent free of charge to Siemens Healthineers MR customers, qualified physicians, technologists, physicists and radiology departments throughout the world. It includes reports in the English language on magnetic resonance: diagnostic and therapeutic methods and their application as well as results and experience gained with corresponding systems and solutions. It introduces from case to case new principles and procedures and discusses their clinical potential. The statements and views of the authors in the individual contributions do not necessarily reflect the opinion of the publisher.

The information presented in these articles and case reports is for illustration only and is not intended to be relied upon by the reader for instruction as to the practice of medicine. Any health care practitioner reading this information is reminded that they must use their own learning, training and expertise in dealing with their individual patients. This material does not substitute for that duty and is not intended by Siemens Healthcare to be used for any purpose in that regard. The drugs and doses mentioned herein are consistent with the approval labeling for uses and/or indications of the drug. The treating physician bears the sole responsibility for the diagnosis and treatment of patients, including drugs and doses prescribed in connection with such use. The Operating Instructions must always be strictly followed when operating the MR system. The sources for the technical data are the corresponding data sheets. Results may vary.

Partial reproduction in printed form of individual contributions is permitted, provided the customary bibliographical data such as author's name and title of the contribution as well as year, issue number and pages of MAGNETOM Flash are named, but the editors request that two copies be sent to them. The written consent of the authors and publisher is required for the complete reprinting of an article.

We welcome your questions and comments about the editorial content of MAGNETOM Flash. Please contact us at
magnetomworld.team@siemens-healthineers.com

Manuscripts as well as suggestions, proposals and information are always welcome; they are carefully examined and submitted to the editorial board for attention. MAGNETOM Flash is not responsible for loss, damage, or any other injury to unsolicited manuscripts or other materials. We reserve the right to edit for clarity, accuracy, and space. Include your name, address, and phone number and send to the editors, address above.

MAGNETOM Flash is also available online:

www.siemens.com/magnetom-world

On account of certain regional limitations of sales rights and service availability, we cannot guarantee that all products included in this brochure are available through the Siemens Healthineers sales organization worldwide. Availability and packaging may vary by country and is subject to change without prior notice. Some/All of the features and products described herein may not be available in the United States.

The information in this document contains general technical descriptions of specifications and options as well as standard and optional features, which do not always have to be present in individual cases.

Siemens Healthineers reserves the right to modify the design, packaging, specifications, and options described herein without prior notice. For the most current information, please contact your local sales representative from Siemens Healthineers.

Note: Any technical data contained in this document may vary within defined tolerances. Original images always lose a certain amount of detail when reproduced.

The outcomes and statements provided by customers of Siemens Healthineers are unique to each customer's setting. Since there is no "typical" hospital and many variables exist (e.g., hospital size, case mix, and level of service/technology adoption), there can be no guarantee that others will achieve the same results.

Siemens Healthineers Headquarters

Siemens Healthineers AG
Siemensstr. 3
91301 Forchheim, Germany
[siemens-healthineers.com](https://www.siemens-healthineers.com)

USA

Siemens Medical Solutions USA, Inc.
Healthcare
40 Liberty Boulevard
Malvern, PA 19355-9998, USA
[siemens-healthineers.us](https://www.siemens-healthineers.us)